

REVIEW ARTICLE

# Biodegradable materials: Foundation of transient and sustainable electronics

**Monisha Monisha, Shweta Agarwala\***

Department of Electrical and Computer Engineering, Finlandsgade 22, Aarhus University, Denmark

## Abstract

Biodegradable materials are designed to degrade in a desired time either through the action of microorganisms or under certain physical conditions. The driving force behind the rise of biodegradable materials is the growing problem of electronic waste (e-waste), low recyclability, and toxicity of electronic materials. Transient response of biodegradable materials has found application in next-generation health-care and biomedical devices. Advances in material science and manufacturing technique have pushed the envelope of innovation further. This review discusses different biodegradable material classes that have emerged to replace the traditional non-biodegradable materials in electronics. Focus has been given to conversion of biodegradable materials to inks and pastes that find use in printed electronics to create flexible, bendable, soft, and degradable devices. Material degradation behavior and dissolution chemistries have been illustrated to understand their impact on electrical performance of devices. Finally, some short-term and long-term challenges are pointed out to overcome the commercialization barrier.

---

**\*Corresponding author:**

Shweta Agarwala  
(shweta@ece.au.dk)

**Citation:** Monisha M, Agarwala S, 2022, Biodegradable materials: Foundation of transient and sustainable electronics. *Mater Sci Add Manuf*, 1(3): 15.  
<https://doi.org/10.18063/msam.v1i3.15>

**Received:** July 31, 2022  
**Accepted:** September 2, 2022  
**Published Online:** September 21, 2022

**Copyright:** © 2022 Author(s). This is an Open Access article distributed under the terms of the Creative Commons Attribution License, permitting distribution, and reproduction in any medium, provided the original work is properly cited.

**Publisher's Note:** Whioce Publishing remains neutral with regard to jurisdictional claims in published maps and institutional affiliations.

**Keywords:** Biodegradable materials; Biodegradable metals; Biodegradable polymers; Transient electronics

---

## 1. Introduction

Technological advancements and ever-increasing reliance on electronic devices have seen an unprecedented increase in the recent times. This has made our life easier, communication faster, and medical devices precise. Simultaneously, it has created an issue of growing electronic waste (e-waste). Just like plastic waste, e-waste takes up the space, releases toxins in the environment, and is not degradable. E-waste is the world's fastest growing waste stream with figures hitting around 74 metric tonnes by 2030<sup>[1]</sup>. Conventional electronics uses inorganic materials, namely, silicon, copper, and gallium arsenide, which degrade through corrosive action. The inorganic metals and ceramics undergo degradation through mediation of surface reactivity, metal catalysis, and resorbability. Most of the inorganic materials form an inert protective layer on exposure to the environment, thus hampering its degradation. Even if the material can be degraded under certain conditions, it often leads to leaching of heavy metal ions, which are toxic to the living organisms and cause environmental issues.

This has led researchers and industries to explore ways of not only recycling existing electronics but also finding viable alternatives to the non-degradable materials used

in electronic chips. Obtaining green materials, eco-friendly fabrication processes, and devices with low embodied energy have become prerequisite for sustainable electronics moving forward. There is a growing need for the development of biodegradable materials that can partially or completely degrade into non-toxic material under normal environmental and physiological conditions. Electronics fabricated using these materials are termed as transient electronics as they disintegrate fully or partially after a certain period of steady operation. The development of biodegradable electronic materials and devices that safely degrade at the end of their life cycle will reduce the financial costs, health care, and environmental risks and streamline the waste management system. The emerging technology of biodegradable electronics has expanded opportunities in many sectors, such as solar cells, batteries, and plant monitoring sensors with main influence being in health care (Figure 1). In this review, we discuss the emergence of biodegradable materials, which have application in electronics. The biodegradable materials, namely, conductors, semiconductors, and insulators and dielectrics, are categorized according to their electrical performance. The paper also discusses emerging functional materials such as inks and pastes that are being used in additive manufacturing and printed electronics. The dissolution chemistry of the materials is discussed in detail with emphasis on the electrical performance. Finally, the review discusses the recent developments in the field of electronics and their end of life and highlights the challenges associated with the biodegradable materials and their applications.

## 2. Biodegradation mechanism

The biodegradation of the materials into its smaller constituents generally involves the process that is either influenced by biotic means that involve microorganisms such as fungi and bacteria or abiotic means that involve hydrolysis, photolysis, or oxidization. In nature, both biotic and abiotic mechanisms exist together and the whole degradation is a sum of both. The degradation of the materials is affected by many factors external (environment) and internal (molecular structure). There are mainly two different types of degradations categorized as biotic and abiotic. Biotic degradation, also referred to metabolic degradation, leads to disintegration of the material through the change in their physicochemical properties through microorganisms. Most materials are degraded by microbial attack in a single step. Biotic degradation is the most significant removal pathway of contaminants from the natural environment. If the biological activity is the predominant influence in the breakdown of a material, then it is referred to as abiotic degradation. The process

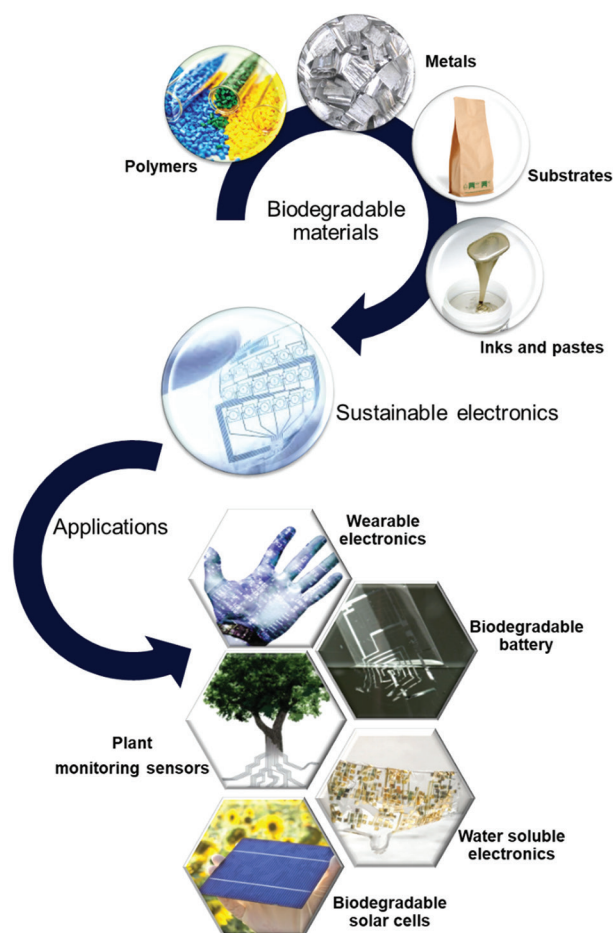


**Figure 1.** Schematic diagram illustrating various categories of biodegradable materials and their application in electronics.

mainly includes hydrolysis and photolysis. Hydrolysis in water is often accelerated by the presence of acids and bases. Photolysis is a light-induced redox reaction, which breaks the constituents wherever the light can reach.

### 2.1. Dissolution chemistry

In studying biodegradable materials, most of the research has been focused on dissolution rates, wherein a material breaks up into smaller group of molecules or constituents in a solvent. In general, investigations on the dissolution rates of biodegradable materials do not involve microorganisms. Research in dissolution chemistry of biodegradable materials involves dissolving them in suitable solvents or hydrolysis in water or biofluids. Dissolution rate of various biodegradable electroactive materials is given in Table 1. The mechanisms and kinetics of dissolution and their reaction products are important for potential application of biodegradable materials in eco-friendly electronics, biomedical devices, and environmental sensors. All the investigations involving degradation of metals follow the

Table 1. Dissolution rate of various biodegradable electroactive materials

Electroactive material	Dissolution rate			References
	DI water	Hanks' solution	PBS buffer	
Mg foil	-	1.08 $\mu\text{m}/\text{day}$	-	[3]
Mg	$1.7 \times 10^3 \text{ nm}/\text{day}$	-	-	[16]
MgO/Mg(OH) <sub>2</sub>	5 – 8 nm/day	-	-	[17]
MgO	~50 nm/h	-	-	[21]
Mg – 1Zn – 0.2 Sr – Mg – 1Zn – 1Sr alloys	-	0.53 – 5.09 mm/year	-	[22]
W foil	-	0.19 $\mu\text{m}/\text{day}$	0.15 $\mu\text{m}/\text{day}$	[9]
W	-	-	300 – 700 $\mu\text{m}/\text{year}$	[23]
ce-WS <sub>2</sub>	-	-	5 – 8 nm/week	[16]
W/MgO/Mg/W-based device	20 min	-	-	[24]
W and Mo oxides	~0.2 – 0.5 nm/day	-	-	[17]
Mo	$(1 \pm 0.1) \times 10^{-3} \mu\text{m}/\text{h}$	-	-	[7]
Mo	7 nm/day	-	2 nm/day	[16]
Mo foil	-	0.005 $\mu\text{m}/\text{day}$	0.02 $\mu\text{m}/\text{day}$	[9]
ce-MoS <sub>2</sub>	-	-	10 – 20 nm/week	[16]
Zn foil	-	7.2 $\mu\text{m}/\text{day}$	3.5 $\mu\text{m}/\text{day}$	[9]
Zn/PVA	5 days	-	-	[25]
ZnNPs/Ag NWs (5 wt%)	40 h	-	-	[26]
ZnO	15 h	-	-	[27]
Zn: PVP: glycerol: methanol (7:0.007:2:1)	25 min	-	-	[28]
Fe foil	-	0.005 $\mu\text{m}/\text{day}$	0.08 $\mu\text{m}/\text{day}$	[9]
Si NM	-	-	5 nm/day	[16]
Si NM	-	-	4.5 nm/day	[29]
Monocrystalline Si NMs	0.2 nm/day	58 nm/day	$4.8 \pm 0.2 \text{ nm}/\text{day}$	[15]
SiO <sub>2</sub>	-	-	14 nm/day	[16]
Poly-Si	2.8 nm/day	-	-	[19]
a-Si	4.1 nm/day	-	-	[19]
SiGe	0.1 nm/day	-	-	[19]
Ge	3.1 nm/day	-	-	[19]
SiO <sub>2</sub>	0.13 nm/h	-	-	[20]
Si <sub>3</sub> N <sub>4</sub>	0.0044 nm/h	-	-	[20]
Silk/PEDOT: PSS	~10 days	-	-	[30]
GG5	~0.85%/day	-	-	[31]
GP: G (0.9:5 – 1.8:2.5)	~0.9% – 0.01%/day	-	-	[31]
PPOMaC 4	-	-	$77.50 \pm 1.93\%$ (10 weeks)	[32]
EPPOMaC 8	-	-	$18.45 \pm 4.44\%$ (10 weeks)	[32]

fundamental mechanisms and consequences which are established through in-depth experiments employing metal films in deionized (DI) water. In every case, majorly three types of changes were observed: (i) Mass loss happens at rates lower than the electrical dissolution rate (EDR), primarily because micropores and/or pits form; (ii) oxides

appear on the surfaces as dissolution products, where they can act as protective layers to slow down the dissolution of underlying metal; and (iii) the formed residual oxide layers dissolve much more slowly than the metal.

Thus, it is important to study the degradation process of metals impacted by dissolution kinetics. Equation I

was suggested by Li *et al.*<sup>[2]</sup> to calculate the rates at which bioresorbable metal degrades.

$$v = \sqrt{kD} \frac{\omega_0 M}{q \rho M_{H_2O}} \tanh \sqrt{\frac{kh_0^2}{D}} \quad (I)$$

Where,  $k$  is the reaction constant,  $D$  is the diffusivity of water phosphate-buffered saline (PBS),  $\omega_0$  is the initial water concentration,  $q$  is the number of water molecules that react with each atom of the material,  $\rho$  is the mass density of the dissolution material, and  $M$  and  $M_{H_2O}$  are the molar mass of the dissolution material and water, respectively. By adjusting the pH of the solution and observing the time-dependent changes in electrical resistance, Rogers *et al.*<sup>[3]</sup> investigated the dissolution rates of several bioresorbable metallic films. The metallic films degraded in DI water and in Hanks' Balanced Salt Solution (HBSS), which has a pH range of 5-8. Chloride ions ( $Cl^-$ ) caused Mg to deteriorate 10 times more quickly in HBSS than in DI water. Regardless of pH or temperature, the presence of  $Cl^-$  ions speeds up the degradation of Mg by removing its surface protective layer<sup>[4]</sup>. Zn exhibits an 8.2, 2.6, and 3.3 times greater EDR in salt solution with pH values of 5, 7.4, and 8, respectively, following the same trend. Zinc hydroxide,  $Zn(OH)_2$ , a metabolite, is produced when zinc oxide ( $ZnO$ ) is solubilized in water<sup>[5]</sup>. In a dissolution test in DI water and at room temperature, conducted by Dagdeviren *et al.*<sup>[6]</sup> it was discovered that 200 nm thick  $ZnO$  vanished entirely in 15 h. W has 4 times higher EDR in salt solution with a pH value ranging from 7.4 to 8 as compared to a solution with pH value of 5. This is attributed to the sensitivity of W toward deposition conditions. The EDR of W deposited using the sputtering technique was higher than the one formed using chemical vapor deposition (CVD). Mo has a greater EDR in DI water than in salt solution, in contrast to Mg and Zn. The greater concentration of dissolved oxygen in aqueous solution is responsible for this difference<sup>[7]</sup>. It showed slower dissolution rates at higher pH in HBSS, as shown in Figure 2A and B<sup>[3]</sup>. Although, Fe has the highest EDR at pH 5, but due to the development of passive oxide layer in DI water, its dissolution ceases after 120 h<sup>[8]</sup>. Within a few days, 300 nm thick oxides on Mg, AZ31B Mg alloy, and Zn completely vanished in DI water, while residual oxides were detected on Mo (40 nm) and W (150 nm) substrate for a few weeks, which makes the degradation process slower<sup>[3,9-11]</sup>. As stated earlier, pure Si is a non-degradable material. However, nanostructured Si may have dissolution kinetics that can be varied. Its dissolution kinetics was studied by monitoring the change in Si nanomembranes (NMs) thickness with time using profilometer or atomic force microscopy (AFM) in bovine serum<sup>[12]</sup>. As shown in Figure 2C and D, a variety of variables, including

pH, temperature, concentration, doping level, and the types of ions and proteins present in the solution, have a substantial impact on the dissolving rates<sup>[12-15]</sup>. Higher temperatures and pH levels were shown to speed up the dissolution process, but doping levels more than  $10^{20} \text{ cm}^{-3}$  had the reverse effect<sup>[12,13]</sup>. Similar to Mg dissolution, the presence of chlorides and phosphates above a certain level at approximately pH = 7.5 accelerates the Si dissolution (Figure 2D)<sup>[14]</sup>. In another study, researchers found that extremely thin Si NMs hydrolyze to form orthosilicic acid,  $Si(OH)_4$ <sup>[16]</sup>. These NMs with variable thickness from 35 to 100 nm dissolve in PBS at 37°C in ~ 8 – 22 days with the approximate rate of 4.5 nm/day<sup>[17]</sup>. The dissolution rate ( $R$ ) of Si at temperature  $T$  with molar concentrations of water and hydroxide ions was given by Equation II<sup>[13,18]</sup>.

$$R = k_0 [H_2O]^4 [OH^-]^x e^{\frac{E_A}{k_B T}} \quad (II)$$

Where,  $k_B$  is the Boltzmann constant,  $E_A$  is the activation energy, and fitted values of  $x$  fall in the range of 0.46 – 0.9. The dissolution rate increased with increase in the pH value. Change in the concentration of PBS solution from 0.05 to 1 M increased the dissolution rate from 10 to 20 times. Besides for Si NMs, above equation can be used to determine the dissolution rate of other semiconducting materials such as polycrystalline amorphous Si (a-Si), Si (poly-Si), Si-Ge alloy (SiGe), and Ge. Their dissolution rate was found to be 4.1, 2.8, 0.1, and 3.1 nm/day, respectively, in a buffer solution of pH 7.4 at 37°C. Studies using molecular dynamics (MD) simulations and density functional theory (DFT) indicated that silicon dissolution initiates by the nucleophilic attack on silicon surface bonds, weakening the inner bonds. This makes them even more prone to subsequent ion attacks<sup>[14]</sup>. The dissolution rates of a-Si, poly-Si, and Ge increased by  $10^2 - 10^3$  times, and those of SiGe increased by 10 times, with a rise in pH from 7 to 10<sup>19</sup>. Kang *et al.*<sup>[20]</sup> examined the  $SiO_2$  and  $Si_3N_4$  dissolving rates in various pH solutions. The room temperature dissolution rates for  $SiO_2$  and  $Si_3N_4$  are around 0.13 and 0.0044 nm/h in a buffer solution of pH = 7.4, respectively. The dissolution rates were increased by one or two orders in magnitude with increase in pH value to 12. Another study found that a 150 nm thick MgO film created using electron beam evaporation may disintegrate in deionized water at a rate of about 50 nm/h<sup>[21]</sup>. Thus, the dissolution rate of metals gets affected by the change in conditions and deposition method of the film.

### 3. Biodegradable conducting materials

#### 3.1. Metals

Metal has widely been used as interconnects and electrodes in electronic devices. They have found their wide usage in

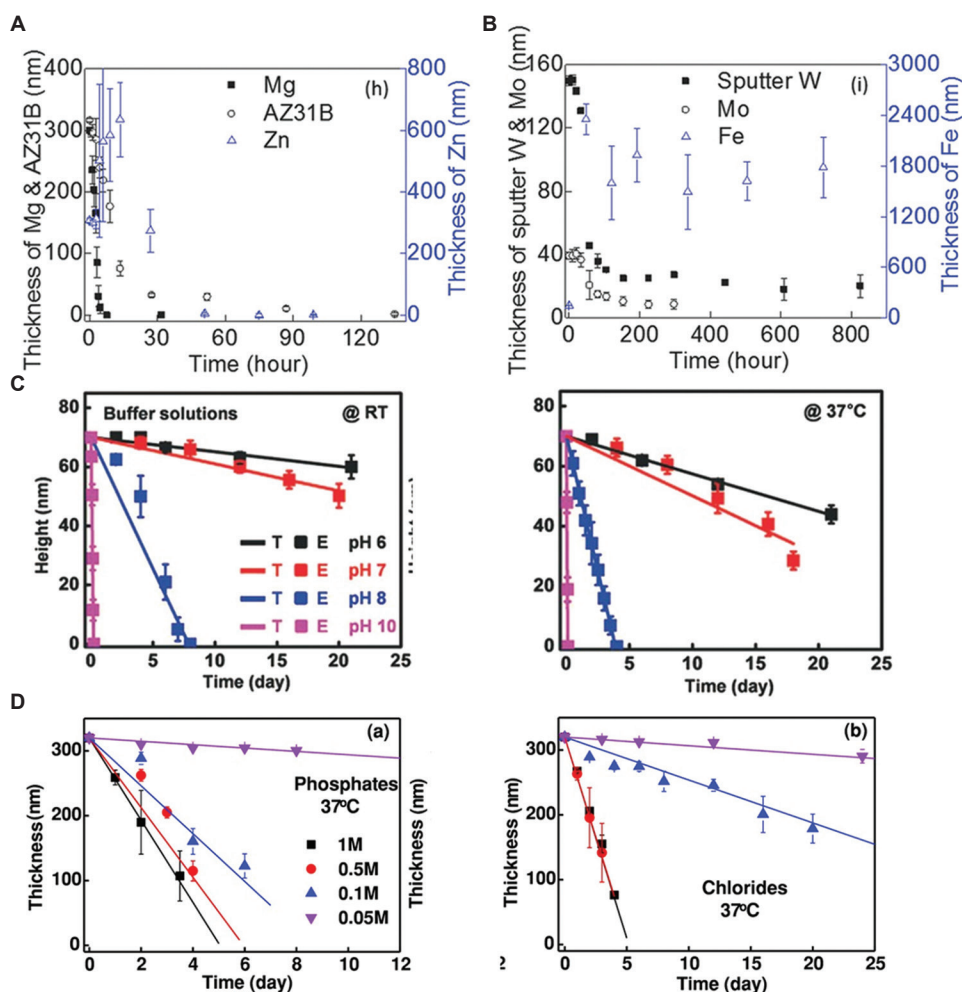


**Figure 2.** Change in thickness of thin films of metals with time during dissolution in DI water at room temperature for (A) Mg, AZ31B Mg alloy and Zn; (B) sputter deposited W, Mo, and Fe; (C) hydrolysis of Si NMs in buffer solutions at different pH at room temperature (left) and at physiological temperature (right, 37°C); and (D) change in thicknesses of Si NMs with time on immersing in aqueous solutions of potassium chlorides and potassium phosphates at 37°C with different concentrations. Reprinted with permission from Yin *et al.*, Hwang *et al.*, and Yin *et al.*<sup>[3,13,14]</sup>.

batteries<sup>[33,34]</sup>, sensors<sup>[35-38]</sup>, implantable stimulators<sup>[39,40]</sup>, and energy harvesters<sup>[41]</sup> (Figure 3A)<sup>[6,42,43]</sup>. Despite this, only few degrade naturally and are considered biodegradable. The metals in aqueous conditions degrade through corrosion, leading to the formation of oxides and hydroxides. For example, metals such as zinc (Zn), iron (Fe), magnesium (Mg), and molybdenum (Mo) undergo degradation through reactions of hydrogen evolution in neutral aqueous media, while tungsten (W) undergoes corrosive process through oxygen absorption in aqueous environment<sup>[23,44-49]</sup>.

Much of the early work on biodegradable metals started with iron, which was used in wire form for implants<sup>[50]</sup>. However, investigations on Fe remain low due to the issue of easy corrosion and slow degradation rate. Mg remains the most sought after biodegradable materials due to its

good mechanical properties and biocompatibility. Much investigations have been carried out on alloys of Mg, namely, Mg-Ca, Mg-Zn, Mg-Si, and Mg-Ag<sup>[22,29]</sup>. Hwang *et al.* used Mg electrodes in silicon-based transient device<sup>[17]</sup>. Later, their group demonstrated uniform dissolution of Mg in DI water with the formation of MgO and Mg(OH)<sub>2</sub> on the surface, which took the shape of nanoneedle-like structures<sup>[3]</sup>. Both the end products have high solubility in water and can be dissolved easily. Recently, research group at University of Glasgow fabricated a transient transistor based on n-channel silicon nanoribbons on Mg as substrate<sup>[24]</sup>. The fabricated transistor performed well with high mobility and high on/off current ratio. They studied the effect of transience on the electrical functioning of the device and observed Mg degradation under different pH. In another report by Cao *et al.*,<sup>[51]</sup> a transient volatile memristor

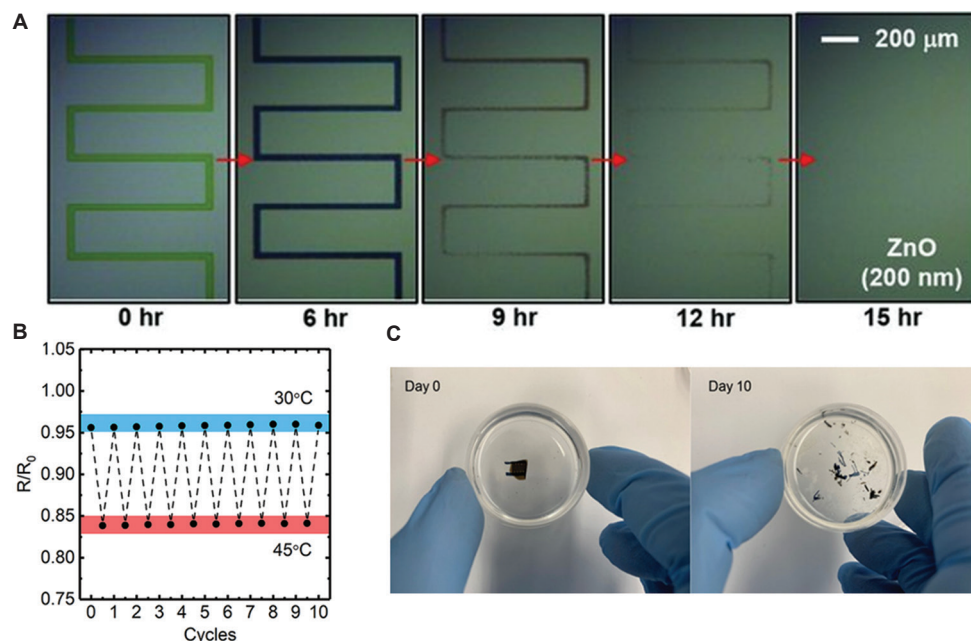


**Figure 3.** (A) A series of optical microscope images were taken at different points during the dissolution of a meander trace of ZnO (200 nm) submerged in DI water at room temperature, (B) changes in the relative resistance of a PEDOT:PSS-based printed temperature sensor subjected to cyclic heating and cooling run between 30°C and 45°C, and (C) the degradation of the flexible temperature sensor over the course of 10 days in an enzymatic (protease) environment. Reprinted with permission from Dagdeviren *et al.*, Wang *et al.*, and Pradhanand and Yadavalli<sup>[6,58,60]</sup>.

device using Mg as an active electrode was fabricated on a polyvinyl alcohol (PVA) substrate. The full degradation of the device was achieved in DI water in about 20 min. Mg-based biodegradable metals have rapid degradation rates, resulting in loss of mechanical performance in short span and thus limiting its applications. Hence, Mg-based biodegradable materials will benefit from decreased degradation rates while Fe may need enhanced rates. Zn is heralded as the next promising metal for biodegradability. Zn-based materials overcome several drawbacks that were observed for other biodegradable materials. Wang *et al.*<sup>[52]</sup> studied mechanical properties of Zn alloy as a degradable biomaterial by casting with Mg. They showed Mg-Zn alloy degradation behaviors in simulated body fluid (SBF) solution. Both Mo and W show slow degradation rates. The variation in degradation rates of metals provides multiple options to use in different applications. Crystalline Zn films with conductivity of approximately  $1.124 \times 10^6$  S/m were produced on a cellulose substrate. The resulting resistive Zn strain gauge array with a gauge factor of  $\approx 1$  exhibited no delamination or cracking, or electrical degradation after repeated stretch-release cycles, and a deflection of  $\approx 16$  mm (radius of curvature) was stably detected<sup>[53]</sup>. It is interesting to note that post-processing method has a considerable effect on the conductivity values of biodegradable metals. Electrochemical sintering process of Zn microparticles was carried out with acetic acid solution, and enhanced

conductivity was observed ( $\approx 3 \times 10^5$  S/m)<sup>[25]</sup>. The conductivity value of  $1.124 \times 10^6$  S/m for Zn was obtained through laser sintering rather than heat sintering. Photonic sintering has also been applied, which resulted in high conductivity value of 44,634 S/m<sup>[48]</sup>. An alternate way of enhancing the conductivity of biodegradable metals is by making the composite with other highly conducting materials. The performance of Zn metal was enhanced by adding small amounts of silver nanowires (NWs), leading to maximum conductivity of 307,664.4 S/m after sintering<sup>[26]</sup>. Nevertheless, adding Ag may compromise the biodegradability of the overall composite.

### 3.2. Polymers

Polymer materials have better biodegradability and biocompatibility than metals and have been much sought after. This is true for both natural and synthetic polymers. Synthetic polymers are particularly attractive as their degradation rates can be tuned through triggered depolymerization. Moreover, polymer materials are cheap and easy to process that make them attractive for commercialization. Organic polymers show conducting properties through introduction of conjugation or doping with conductive materials. Examples of conjugated polymers are polyaniline (PANI), polypyrrole (PPy), and poly(3,4-ethylenedioxythiophene) (PEDOT). The conjugated network in conductive polymers makes

them brittle and inflexible, which can be overcome by doping the conjugated polymers without affecting their electrical properties<sup>[54-56]</sup>. PEDOT: PSS, a polymer doped with poly(styrenesulfonate) (PSS), shows the best known conductivity of up to  $4.6 \times 10^5$  S/m in polymeric materials<sup>[57]</sup>. This electrode was developed by Worfolk *et al.*<sup>[58]</sup> to fabricate a sensor with a sensing range from 30°C to 45°C (Figure 3B).

Another strategy to tune degradability is to blend conducting polymers with biodegradable polymers to achieve partial degradation. Partial degradation is achieved, as these polymers do not break down completely into monomers. Shi *et al.* used a composite of PPy nanoparticles (NPs) with poly(D,L-lactic acid) (PDLLA), where NPs formed a conductive network within the PDLLA matrix for fibroblast growth. Adding even a small amount of PPy leads to high conductivity (approximately  $1 \times 10^{-3}$  S/cm), with the material being stable for about 1000 h<sup>[59]</sup>. Similarly, Wang *et al.*<sup>[30]</sup> used a combination of hyaluronic acid (HA)-doped PEDOT (10% NP loading) with poly(L-lactic acid) (PLLA) to fabricate a conductive film. The degradation of PLLA was accelerated by PEDOT-HA by almost 10%. The enhanced degradation can be assigned to increased water penetration in PLLA due to the presence of hydrophilic HA.

In another work, a mixture of PEDOT: PSS with photosericin and Irgacure 2959 photoinitiator was synthesized to prepare a conducting material. The fabricated sensor showed a high sensitivity ( $-0.99\% \text{ } ^\circ\text{C}^{-1}$ ) in the temperature range of 20 – 50°C and excellent stability on exposure to about 60% relative humidity. The sensor was degradable in approximately 10 days under proteolytic conditions (Figure 3C)<sup>[60]</sup>. Hybrid approaches have also been investigated to realize fully degradable materials wherein inorganic materials are mixed with organic materials. In one report, Si NPs were mixed with carbon black and PEDOT: PSS to make electrodes for lithium-ion battery application<sup>[61]</sup>.

Li *et al.*<sup>[62]</sup> reported electrospun camphor sulfonic acid (CPSA) doped with PANI and gelatin to obtain high conductivity material (up to  $2.1 \times 10^{-2}$  S/cm). In another report, CPSA/PANI composite was doped with poly(L-lactide-co-ε-caprolactone) and showed high conductivities (up to  $1.38 \times 10^{-2}$  S/cm). Electrical stimulation through these conducting fibers showed increased adhesion and proliferation for fibroblasts and myoblasts cells<sup>[63]</sup>. Hydrogels obtained by grafting PANI with gelatin and doping with CPSA exhibited conductivities around  $10^{-4}$  S/cm<sup>[31]</sup>. P3HT was electrospun with polycaprolactone (PCL)<sup>[40]</sup> and polylactic-glycolic acid (PLGA)<sup>[64]</sup> to introduce partial degradability. The resulting electrospun nanofibers with PCL, however, displayed lower

values of mobility ( $1.7 \times 10^{-2}$  cm<sup>2</sup>/V.s) due to macroscopic phase segregation.

### 3.3. Inks and pastes

The emerging field of printed electronics, an additive manufacturing technology, has opened doors to directly write electronic materials on desired substrates. The technology requires the materials to be converted to functional inks and pastes to be printed through inkjet, aerosol jet, screen printing, pneumatic head, or laser-based techniques. Hence, many conducting metals have been dissolved in aqueous, polar, or non-polar solvents to convert to inks. Biodegradable inks differ in particle size, types of additives, and solvent. In general, the biodegradable inks are made up of three key ingredients, namely, nanoparticles, small quantity of polymers as stabilizers, and suitable solvent. Mahajan *et al.*<sup>[65]</sup> prepared a stable conductive ink by dispersing Zn NPs (of average diameter 50 nm) with PVP particles in a solvent mixture of methanol and butyl acetate. In another work, Zn NPs were mixed with Ag NWs and polyethylene oxide (PEO) to prepare the ink<sup>[26,66]</sup>. Addition of Ag NW also adds a stretchable character to the printed patterns. Most of the prepared inks and pastes were processed using printed techniques such as screen printing, inkjet, and aerosol printing. To create a uniform dispersion of the biodegradable material particles, polymers are used as additives. Most of the additives, however, are insulating in nature and could hinder electron transport. Thus, it is important to post-process the printed patterns by heat sintering to degrade the additives. Huang *et al.*<sup>[67]</sup> prepared a W paste with PEO particles as additives in methanol. As stated earlier, most metal-based biodegradable materials are brittle at room temperature and, thus, require some sort of post-processing to enhance the mechanical properties. Li *et al.*<sup>[66]</sup> improved the conductivity of the Zn ink by an improved water sintering method. This ink showed the capability to withstand 1500 repeated bending test with a curvature of 3.8 mm. In another study, an ink based on Zn and Ag NW composite exhibited a high conductivity with excellent mechanical using the same water sintering approach. The authors demonstrated that the printed patterns were robust and could withstand 8000 bending cycles<sup>[26]</sup>.

## 4. Biodegradable semiconducting materials

### 4.1. Inorganic semiconductors

Semiconductors have a bandgap, and their electrical conductivity is between conductors and insulators. They play a major role in fabrication of the electronic devices. Present electronic industry is based on silicon (Si) semiconductor, which is used in various forms to make devices, namely, monocrystalline silicon

(mono-Si)<sup>[68]</sup>, amorphous silicon (a-Si)<sup>[69]</sup>, polycrystalline silicon (poly-Si)<sup>[70]</sup>, and silicon alloys<sup>[71]</sup>. The various Si forms used in the present day do not degrade due to the formation of a native oxide layer on top, which renders them chemically inert. Research has been focused toward increasing the hydrolysis rate of Si by reducing their thickness and aspect ratio to make nanostructures<sup>[72]</sup>. The hydrolysis of Si in water results in the formation of orthosilicic acid ( $\text{Si}(\text{OH})_4$ )<sup>[72]</sup>. Most of the work has been done on Si-NM. Hwang *et al.*<sup>[12]</sup> carried out detailed investigation on the dissolution behavior of Si-NM nanostructures on silicon dioxide/silicon substrate through observing thickness change against time (Figure 4A). Through various reported literature, it has been established that the dissolution kinetics of Si NM depends on physical factors such as microstructure, geometry, and surface conditions and on external factors such as pH and temperature<sup>[12,73,74]</sup>. Effect of pH on Si NM has been widely investigated, where Yin *et al.*<sup>[55]</sup> found that the higher concentration on  $\text{OH}^-$  ions in the solution led to faster dissolution. The group also explained the weakening of Si-Si backbones in the material through nucleophile ions being bonded to Si surface. Si-NM shows promising results in enabling a Si-based material that can be degraded under various conditions. Silicon-

germanium alloys have also shown dissolution in varying pH and temperature ranges<sup>[73,75]</sup>. Increased pH led to reactions that produced metagermanic acid ( $\text{H}_2\text{GeO}_3$ ) on hydrolysis.

Inorganic oxides such as magnesium oxide (MgO), zinc oxide (ZnO), and silicon dioxide ( $\text{SiO}_2$ ) have also been explored in biodegradable electronics due to their superior thermal and chemical stability. The rationale is to keep the material layers thin for better dissolution, as they are dissolvable in aqueous solutions. The dissolution rates depend on many physical and chemical properties and external factors such as pH, temperatures, and ion concentration in the solution<sup>[9,17]</sup>.

## 4.2. Organic semiconductors

Although organic semiconductors have inferior electrical properties compared to their inorganic counterparts, they have the advantage of faster dissolution. Madrigal *et al.*<sup>[76,77]</sup> prepared a composite film from poly(3-thiophene methyl acetate) (P3TMA) by blending with thermoplastic polyurethane (TPU). The composite film demonstrated semiconducting behavior with a wide bandgap ( $\sim 2.35$  eV). However, due to the non-degradability of P3TMA, the film was only partially degradable. A fully biodegradable semiconducting film (PDPP-PD) was

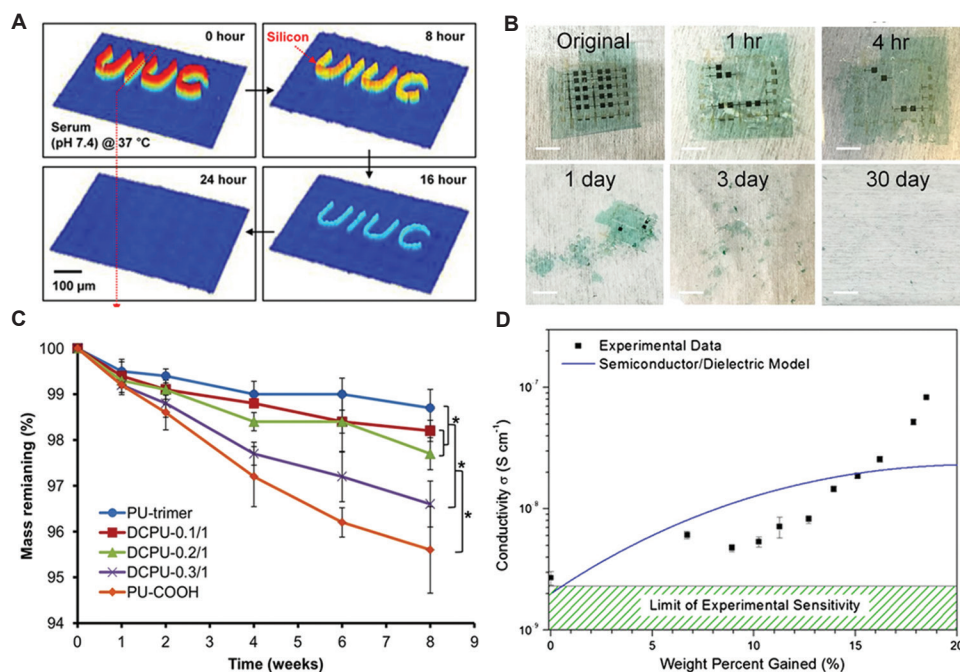


**Figure 4.** (A) Images of Si NMs at different stages of dissolution in bovine serum (pH 7.4) at physiological temperature (37°C) were measured using laser diffraction phase microscopy (DPM): 0 h (top left), 8 h (top right), 16 h (bottom right), and 24 h (bottom left). (B) Photographs of a totally disintegrable device prepared using PDPP-PD semiconducting film at various stages of disintegration (scale bars: 5 mm). (C) Mass remaining for DCPU in PBS at 37°C. (D) Change in conductivity of melanin with water content. The measured humidity was transformed into the percentage of weight gained due to water absorption. Reprinted with permission from Hwang *et al.*, Lei *et al.*, Xu *et al.*, and Mostert *et al.*<sup>[12,78–80]</sup>.

prepared by introducing reversible imine linkages between diketopyrrolopyrrole (DPP) and p-phenylenediamine. The conjugation along the backbone of this polymeric film allows for hole conduction. The degradation of the material takes place through breaking of imine bonds under acidic conditions to give aldehyde and amine precursors as the by-products (Figure 4B)<sup>[78]</sup>. Xu *et al.* reported a polyurethane-based conductive elastomer (DCPU) based on PCL, which used dopant as dimethyl propionic acid and aniline trimer linkers. The conductivity of the synthesized polymer could vary between  $10^{-8}$  and  $10^{-5}$  S/cm in the dry state. Depending on the concentration of dopant present in the polymer, conductivity could be enhanced further on soaking in PBS. Due to the presence of hydrophilic carboxylic functional groups, with the increase in DMPA content, degradation rate increased in aqueous PBS solution. The polymer degraded to ~75% of its weight in 14 days in PBS and in the presence of lipase without any decline in conductivity during degradation period (Figure 4C). The chemical linkage in the matrix helps to stabilize the dopant and leads to improved electronic performance<sup>[79]</sup>. Natural pigments<sup>[80,81]</sup>, conjugated molecules such as *Indigofera tinctoria* and *Isatis tinctoria*<sup>[82]</sup>, melanin, and  $\beta$ -carotene<sup>[83,84]</sup> have also been explored for the preparation of biodegradable electronics. Some natural semiconductor materials include indigo with a band gap of 1.7 eV and decent carrier mobilities. Eumelanin, a subclass of melanin, also exhibits electronic behavior. Conductivity of melanin depends on temperature, its hydration state, and physical form. Mostert *et al.*<sup>[80]</sup> demonstrated that eumelanin conducts free electrons and protons for electronic and ionic conduction, respectively, after absorption of water molecules, as shown in Figure 4D. The material was used as a regenerative medical scaffold, which could resorb in about 8 weeks<sup>[81]</sup>.

Fully biodegradable conducting polymers can be prepared by interrupting the conjugation with the introduction of flexible non-conjugated linkers in the polymer backbone. This process makes the polymers flexible and processing easy, but decreases the conductivity as compared to partially degradable conductive polymers<sup>[31,79,85,86]</sup>. Due to the intrinsic flexibility of the material, these polymers are used in sensors as interconnects where low conductivity is not an issue. Electrical stimulation to promote cell growth and tissue regeneration of scaffolds and muscle tissues is another application of low conducting polymers<sup>[86-88]</sup>. There is a need to develop new chemistries and increase the conductivity of polymers to fabricate high-performance degradable electronics. Conductivities of various biodegradable conducting materials are given in Table 2.

## 5. Biodegradable dielectrics

When an electric field is present, dielectric polymers, which are insulators, can become polarized. The dielectric constant ( $\kappa$ ), which can be high or low depending on the application, determines polarization. High- $\kappa$  fillers can be added to a degradable polymer matrix to produce biodegradable dielectrics (Table 3). Common high- $\kappa$  metal oxides include aluminum oxide ( $\text{Al}_2\text{O}_3$ ,  $\kappa = 9$ ), silicon oxide ( $\text{SiO}_2$ ,  $\kappa = 3.9$ ), and hafnium oxide ( $\text{HfO}_2$ ,  $\kappa = 25$ ).  $\text{Al}_2\text{O}_3$  was combined with cellulose acetate (CA), and Figure 5A shows that this combination produced a higher  $\kappa$  value of 27.57 at a low frequency of 50 Hz<sup>[93]</sup>. Besides metal oxides, carbon nanotubes also improved the  $\kappa$  of biodegradable paper made from cellulose nanofibers (CNFs) from ~ 0 to 3198 at 1 kHz<sup>[94]</sup>.

Plant-based fibers such as cotton, bamboo, jute, and banana fibers also possess dielectric properties, as shown in Figure 5B<sup>[95-100]</sup>. This is because there are free hydroxyl functional groups present, which add polarity and provide high  $\kappa$  values. Cotton exhibits a dielectric constant of 17 between frequency range of 60 and 1000 Hz<sup>[101]</sup>. Banana, bamboo, and jute fibers were also used as fillers into dielectric composites. The dielectric constant of these composites was found to be increasing with increase in fiber content<sup>[102]</sup>. Natural sugars also behave as dielectrics. High breakdown voltages of 1.5 MV/cm and 4.5 MV/cm, low loss tangents on the order of  $10^{-2}$  at 100 mHz, and dielectric constants of 6.35 and 6.55 at 1 kHz, respectively, are all characteristics shown by glucose and lactose<sup>[84]</sup>.

Besides natural materials, synthetic materials also exhibit biodegradability. An example of synthetic biodegradable dielectric elastomer is poly(glycerol sebacate) (PGS). Such elastic materials are useful for capacitive sensors since they can withstand compression more effectively and thus can be a useful alternative to viscoelastic polymers. Boutry *et al.*<sup>[103]</sup> reported a degradable capacitive pressure sensor fabricated using PGS as the dielectric sandwiched between biocompatible Mg and Fe metal electrodes. Fabricated sensor showed excellent time response while detecting small weights of single grain of salt weighing only 5 mg (Figure 5C). It is important to note that most of the dielectrics mentioned in this review were investigated at frequencies lower than few kHz. For practical use of these biodegradable dielectrics in complex electronic devices, their optimization is required for high-frequency performance.

## 6. Biodegradable insulators

### 6.1. Substrates

Substrates typically constitute most of the weight and volume of an electronic device. Therefore, overall

**Table 2. Conductivities of various biodegradable conducting materials**

Electroactive material	Conductivity	References
Mg	3.4 mS/cm	[33]
W: methanol: PEO (4:1:0.25)	5200 S/m	[67]
Zn NPs/Na-CMC	$1.124 \times 10^6$ S/m	[89]
Zn/PVA	$9.7 \times 10^5$ S/m	[25]
Zn/PVA	$\sim 2 \times 10^6$ S/m	[90]
Zn NPs/PVP (0.1 wt%)	22,321.3 S/m	[65]
Zn NPs/PEO (3 wt%)	72,400 S/m	[66]
ZnNPs/Ag NWs (5 wt%)	307,664.4 S/m	[26]
Zn: PVP: glycerol: methanol (7:0.007:2:1)	60,213.6 S/m	[28]
PEDOT: PSS	$4,600 \pm 100$ S/cm	[56]
10% PEDOT-HA/PLLA	$0.47 \pm 0.21$ S/cm	[59]
30% PEDOT-HA/PLLA	$2.58 \pm 1.02$ S/cm	[59]
50% PEDOT-HA/PLLA	$6.94 \pm 1.23$ S/cm	[59]
Silk/PEDOT: PSS		[30]
Pani: gelatin (0:100 – 60:40)	0.005 – 0.021 S/cm	[62]
CPSA-PANI: PLCL nanofiber (0:100 – 30:70)	0.0015 – 0.0138 S/cm	[63]
GG5	$1.21 \times 10^{-4}$ S/cm	[31]
GP: G (0.9:5 – 1.8:2.5)	$2.41 \times 10^{-4}$ – $4.54 \times 10^{-4}$ S/cm	[31]
Aligned PLGA-PHT nanofibers	$0.1 \times 10^{-5}$ S/cm	[64]
Random PLGA-PHT nanofibers	$0.2 \times 10^{-6}$ S/cm	[64]
TPU: P3TMA	$2.23 \times 10^{-5}$ – $5.19 \times 10^{-6}$ S/cm	[77]
PU-trimer	$2.7 \pm 0.9 \times 10^{-10}$ S/cm	[79]
DCPU-0.1/1	$5.5 \pm 0.7 \times 10^{-8}$ S/cm	[79]
DCPU-0.2/1	$4.6 \pm 0.4 \times 10^{-7}$ S/cm	[79]
DCPU-0.3/1	$1.2 \pm 0.3 \times 10^{-5}$ S/cm	[79]
PU-COOH	$5.5 \pm 1.2 \times 10^{-12}$ S/cm	[79]
Melanin films	$7.00 \pm 1.10 \times 10^{-5}$ S/cm	[81]
2a-PCL EMAP copolymer	$5.01 \times 10^{-6}$ S/cm	[85]
3a-PCL EMAP copolymer	$2.42 \times 10^{-5}$ S/cm	[85]
DNA/HA/SWCNT (0.5/0.3%)	$128 \pm 15$ S/cm	[91]
GelMA/DNA/MWCNT (3/4/6 mg)	$24 \pm 1.8$ S/cm	[91]
Graphene nanoflake ink	$0.43 \times 10^5$ S/m	[92]

degradation behavior of the electronic device largely depends on the substrate used. Researchers are exploring polymers from natural<sup>[91,104-110]</sup> and synthetic sources to be used as substrate. Biodegradable polymers that work as excellent substrate materials include polylactic acid (PLA), PLGA (Figure 6A), PVA (Figure 6B), polyglycolic acid (PGA), poly (1,8-octanediol-co-citrate) (POC), silk fibroin, rice paper, and cellulose nanofibril paper<sup>[10,17,111-113]</sup>. POC was used to fabricate stretchable Si-based pH and electro-physiological sensors using transfer printing. After 12 h, these sensors completely

disintegrated in PBS (pH 10) at ambient temperature, as shown in Figure 6C.<sup>[111]</sup>

By adding maleic anhydride, these elastomers can be rendered photo-cross-linkable, preventing lengthy thermal condensation curing. This method helps increase the variety of materials that can be used as stretchy and biodegradable substrates<sup>[32,114,115]</sup>.

Similarly, silk or its bioresorbable protein fibroin has demonstrated promising applications in electronic devices such as drug delivery systems<sup>[27,116-118]</sup>, wireless therapeutic

Table 3. Dielectric properties of various biodegradable materials

Material	Dielectric constant (1 kHz)	Breakdown field (MV cm <sup>-1</sup> )	Loss tangent (100 mHz)	References
Adenine	~3.85	~1.5	~4 × 10 <sup>-3</sup>	[84]
Guanine	~4.35	~3.5	~7 × 10 <sup>-3</sup>	
Glucose	~6.35	~1.5	~5 × 10 <sup>-2</sup>	
Lactose	~6.55	~4.5	~2 × 10 <sup>-2</sup>	
Sucrose	-	>3	~8 × 10 <sup>-2</sup>	
Caffeine	~4.1	~2	~9 × 10 <sup>-2</sup>	
SiO <sub>2</sub>	~3.9	~5-15	-	
CA <sup>a</sup>	8.63	-	0.26	[93]
CA/Al <sub>2</sub> O <sub>3</sub> (25 wt%) <sup>a</sup>	27.57	-	0.64	
CNF	-	0.6138	-	[94]
CNF/CNT (4.5 wt%)	-	0.4258	-	

<sup>a</sup>Dielectric constant at 50 Hz.

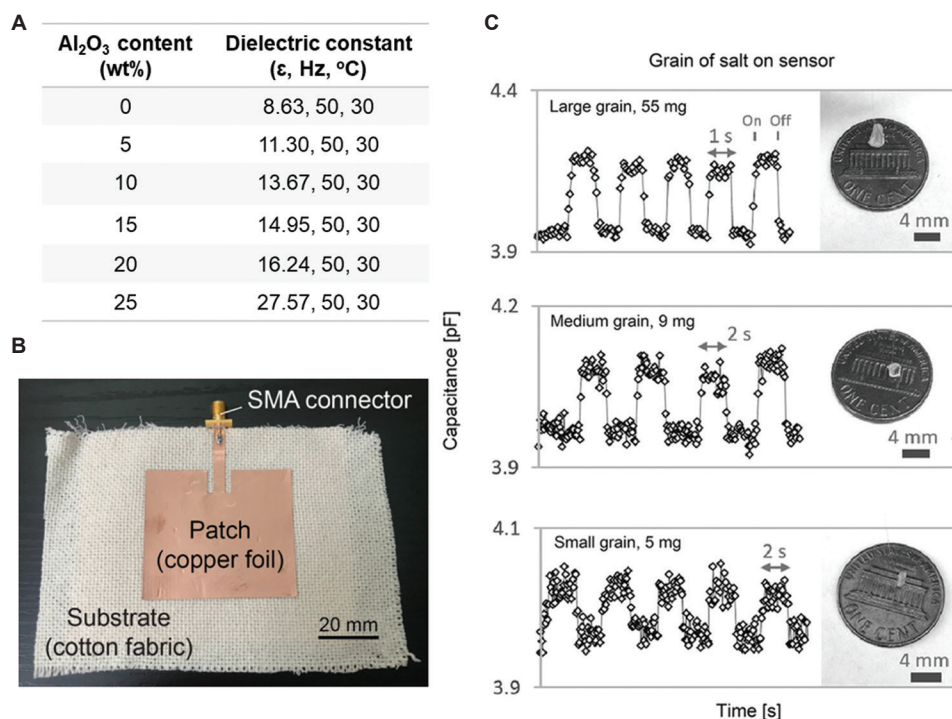


**Figure 5.** Increase in dielectric constant of cellulose acetate with increase in the addition of high-κ additives, Al<sub>2</sub>O<sub>3</sub>, (B) antenna sample using cotton fabric as the substrate and the dielectric material, and (C) a sensor array of 4 × 5 pressure-sensitive elements that can quickly respond to detect the presence of a grain of salt (weights: 55, 9, and 5 mg). Figure (A) is adapted from Deshmukh *et al.*<sup>[93]</sup> Reprinted with permission from Mukai *et al.* and Boutry *et al.*<sup>[95,103]</sup>.

devices<sup>[117]</sup>, energy harvesters,<sup>[6,41,119-121]</sup> and transistors<sup>[17]</sup>. Silk in water degrades at a well-characterized rate that can be easily adjusted by several orders of magnitude by regulating the degree of crystallization. Although highly crystalline silk degrades gradually, it can be fragile and challenging to handle. While less crystalline silk is more flexible, it

breaks down more quickly in water. This trade-off restricts the manufacture of devices using transfer printing on silk substrates. Hwang *et al.*<sup>[13,17]</sup> fabricated Si-based microheaters for transient thermal therapy on silk using transfer printing method. These devices degrade after 15 days to prevent infections after surgery (Figure 7A and B).

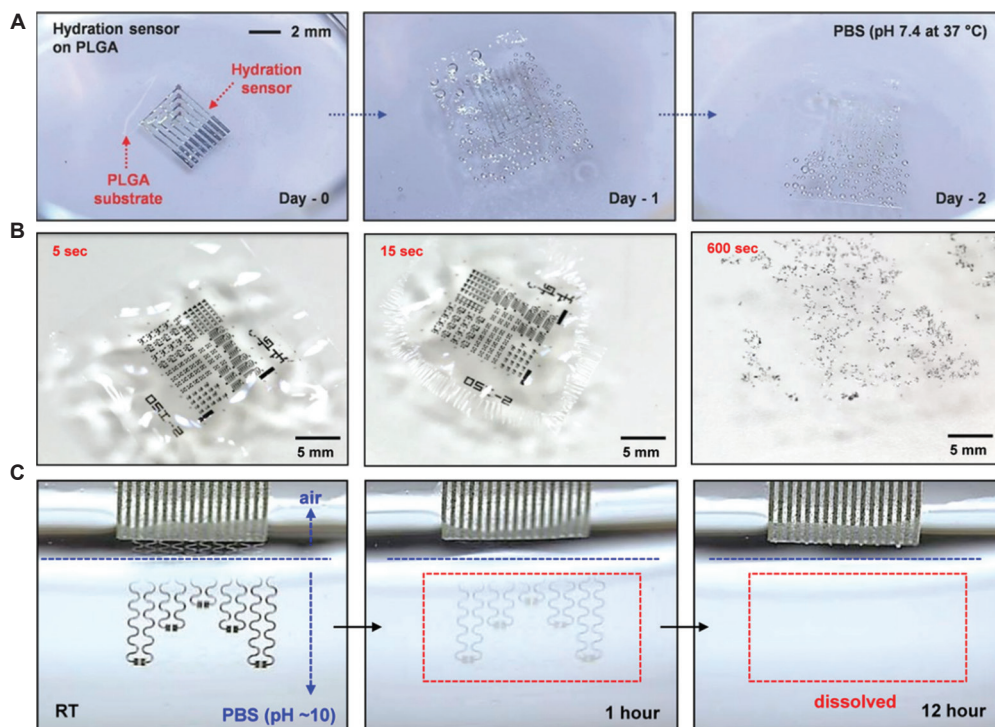


**Figure 6.** (A) Photographs taken at various stages of the dissolution of a transient hydration sensor on a PLGA film while being immersed in PBS (1 M, pH = 7.4) at physiological temperature at 37°C; (B) a collection of optical microscope photographs taken throughout the dissolution of a-IGZO devices in DI water at room temperature. After 1800 s, the PVA substrate completely dissolves, causing the electronic devices to completely dissociate in the water. (C) A sequence of photos showing the breakdown of a POC-modified Si-based device in room temperature PBS (pH = 10). Reprinted with permission from Hwang *et al.*, Hwang *et al.*, and Jin *et al.* [10,111,113].

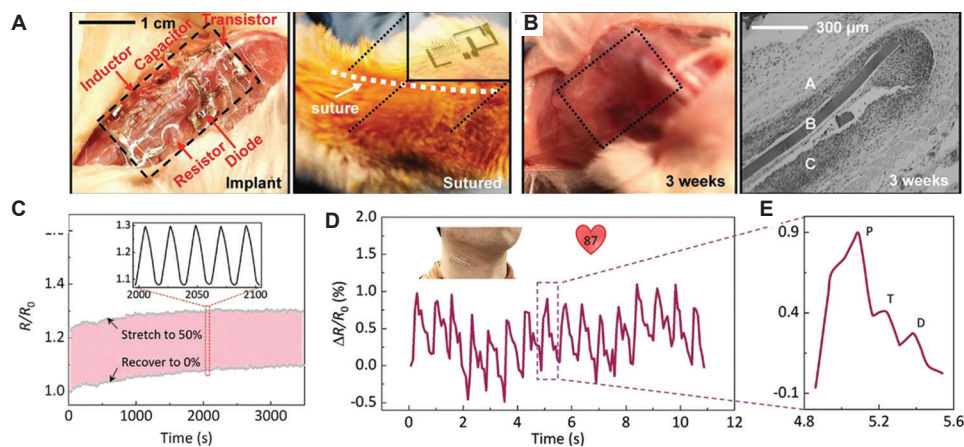


**Figure 7.** An example of a transient bioresorbable device for thermal therapy, together with *in vivo* evaluations. (A) Images of a demonstration platform for transient electronics implanted (left) and sutured (right) in a BALB/c mouse's subdermal dorsal area. (B) The implant location after 3 weeks (left); an implant site histological section that was removed 3 weeks later reveals a partially resorbed area of the silk film (right); pointers A, B, and C indicate subcutaneous tissue, silk film, and muscle layer, respectively. (C) Relative resistance changes of the gelatin-alginate-based strain sensor under cyclic stretching with 50% strain in air (150 cycles); (D) strain sensor attached to volunteer's neck to detect pulse. (E) The magnified graph corresponding to one cardiac cycle with discernible P-wave, T-wave, and D-wave. Reprinted with permission from Hwang *et al.* and Hao *et al.* [13,141].

Plant-based polymers like cellulose, on the other hand, are flexible, transparent, robust at high temperatures, and degrades slowly (on the order of months) when

exposed to fungi that are found in nature, making it a good choice for consumer electronics. Cellulose has been used in solar cells [122-124], organic light-emitting

diodes (OLEDs)<sup>[125]</sup>, sensors<sup>[126-128]</sup>, transistors<sup>[129-132]</sup>, bio-batteries<sup>[133]</sup>, and radiofrequency identification (RFID) antennas<sup>[92,134,135]</sup> as substrate. CNFs were also used to fabricate biodegradable and flexible devices using transfer printing method. Good thermal stability of the material made direct printing possible on CNF papers<sup>[112,136]</sup>. Hsieh *et al.*<sup>[137]</sup> successfully printed and annealed conductive silver lines on CNF papers, thus demonstrating its full potential for roll-to-roll manufacturing. Despite easy availability of natural materials, such materials possess limitations for the wide applications due to high variation in quality from batch to batch. These variations affect the working of the electronic devices. The use of synthetic polymers is one of the solutions to mitigate such issues. Synthetic polymers can be chemically engineered for better control of physical and chemical properties. A combination of PLA and PGA in different ratios gives bioresorbable polymer with tunable mechanical strength and controlled degradation time<sup>[138]</sup>. PVA<sup>[25,28,66,90,113]</sup>, PGS-PCL<sup>[139]</sup>, and sodium carboxymethyl cellulose (Na-CMC)<sup>[65,67,89]</sup> with diverse mechanical and degradation capabilities have been employed due to the various needs for biodegradable healthcare devices. According to a study, numerous bio-based polymer substrate types can be used for printed electronic applications. Compared to conventional PET film, screen printed silver on cellulose acetate propionate (CAP) showed 18% lower resistance value and, hence, better electrical properties<sup>[140]</sup>. Hao *et al.*<sup>[141]</sup> developed a multifunctional gelatin-alginate hydrogel-based soft sensor with improved sensing performance. The degradable sensor is able to sense very small changes in strain, temperature, heart rate, and pH and has also been explored for drug delivery application. Since the device is both degradable and recyclable, it can be reconstructed with new functions (Figure 7C-E). A polymer of methyl 1H-pyrrole-3-carboxylate monomer (“MPC polymer”) was explored as energy storage material for supercapacitors. This polymer, both as a planar electrode and as a composite porous electrode with PLLA, demonstrated charge storage ability that was comparable to that of the pseudocapacitive conducting polymer PPY. In aqueous environment (37°C, pH 8.2), its application in a supercapacitor with an organic electrolyte revealed detectable evidence of deterioration in 8 h.<sup>[142]</sup>

Stimuli-responsive polymeric materials offer various transient modes in aqueous solutions and in ambient atmosphere with precise control over the start of degradation. These materials include temperature-sensitive cyclododecane (CDD) and methanesulfonic acid/wax<sup>[11]</sup>, moisture responsive polyanhydrides<sup>[143,144]</sup>, and photoacid generator/cyclic poly(phthalaldehyde) (PAG/cPPA) that respond to ultraviolet light<sup>[145]</sup>. To ensure

that a gadget performs as intended for a particular amount of time, slow swelling polymers are preferred. Thus, metallic substrates serve as a good alternative option as they do not swell in biological fluids and, therefore, offer dimensional stability. The dissolution rate of thin foils of Fe, Mo, W, and Zn in PBS (pH 7.4 at 37°C) as substrates for transient electronics was found to be 0.08, 0.02, 0.15, and 3.5  $\mu\text{m}/\text{day}$ <sup>[9]</sup>, respectively.

## 6.2. Encapsulating materials

Depending on the intended use, desired device operational times may range from a few days to a few weeks or years. Such time frames are crucial for application in healthcare or clinical settings. Most of the printed electronic devices need to be protected through an encapsulation layer. Thus, selection of the right material for the encapsulation is paramount to achieve biodegradability. The electrically active components may quickly deteriorate in the presence of a high water permeation rate. When exposed to PBS at room temperature, Mg thin film enclosed in 5 m PLGA degrades within 10 min<sup>[15]</sup>. Tuning the physical and chemical properties of biopolymers, such as composition, thickness, crystallinity, and chemistry, can extend the lifetime. A carefully formulated polyanhydride allows the intracranial pressure sensor to operate steadily for up to 3 days<sup>[146]</sup> and silk fibroin with high crystallinity can extend the Mg thin film's lifetime to about 90 h<sup>[17]</sup>. An alternative option is the use of dissolvable oxides, although care should be taken to not use single-layered oxides. Depending on the deposition conditions, single-layer oxide quickly dissolves due to the presence of pinholes. In PBS, Mg with a 200 nm SiO<sub>2</sub> encapsulation dissolves within 1 min, but Mg that has layers of alternate SiO<sub>2</sub> and Si<sub>3</sub>N<sub>4</sub> can last up to 10 days. According to the encapsulation studies for OLED devices, combining oxide layers and biopolymers is projected to significantly extend functional durations<sup>[147]</sup>. In addition, recent research has demonstrated that using a mono-Si thin film (1.5 mm) as the encapsulation layer can greatly increase the device's operating lifetime. Materials coated with Si NMs, such as Mg thin film, maintain their integrity after 60 days in PBS at 37°C<sup>[15]</sup>.

## 7. Biodegradable and transient electronics

The field of biodegradable electronics falls under “green” electronics with the aim to develop electronic components and systems that have degradation and bioresorbability characteristics. Such systems should have degradation of over 80% in the presence of aqueous medium, temperature, humidity, oxygen, microorganisms, or radiations and should ideally convert to harmless substances. Bioresorbability is a subclass of biodegradability that refers to the safe breakdown of the material in the human body after performing its

function, thus obviating the need of physical removal. The first report on transient electronics was published by Hwang *et al.*<sup>[17]</sup> in 2012, where a platform technology was demonstrated. Since then, much research has been focused on developing biodegradable materials for electronic systems, investigating material degradation behavior and dissolution chemistries, modeling degradation, and creating fabrication techniques. Numerous biodegradable devices that operate reliably for a certain amount of time have been demonstrated for environmental applications, hardware security applications, and other applications such as biomedical implants and energy storage devices. Some of the examples for biomedical devices are implantable transient silicon-based devices with microheaters for thermal therapy<sup>[17]</sup>, pressure and temperature sensors for the treatment of brain surgery and monitoring of cardiovascular activities<sup>[146]</sup>, hydration sensors for wound healing applications<sup>[10]</sup>, pH sensors<sup>[111]</sup>, and devices for drug delivery applications<sup>[117,148,149]</sup>. Transient electronics protect the environment by reducing electronic waste. Some recent studies have focused on enzymatic degradation of PEDOT: PSS polymer<sup>[150]</sup> and development of an all-carbon thin-film paper-based transistor, which is 95% recyclable<sup>[151]</sup>. To make transient electronics self-sufficient, the development of transient batteries is a prerequisite. In 2017, Zn-Cu galvanic cell was used to power a temperature sensor and a wireless communication device in the gastrointestinal tract of pigs<sup>[152]</sup>. Recently, a one-dimensional battery, consisting of chitosan as separator, MnO<sub>2</sub> as cathode and a fiber conductor coated with polydopamine/polypyrrole composite material as anode, was developed. Due to its high flexibility, it could be easily injected into the body to power a biosensor<sup>[153]</sup>. To further extend the application, Mg-Mo-based battery was used in wearable electronics to power an electronic watch and wearable health-care devices for electromyography applications<sup>[154]</sup>. Transient electronics are particularly useful for hardware secured devices containing sensitive information. For the purpose, an MgO-based device was developed which can degrade within 8 min in the presence of DI water at room temperature<sup>[155]</sup>. Similarly, a CsPbBr<sub>3</sub>-based device was capable of dissolving in DI water within 60 s<sup>[156-158]</sup>. Focus has also been directed to develop high-performance degradable printed circuit boards (PCBs). In one of the early works, Huang *et al.* demonstrated transient PCB using different materials that dissolved into benign end products on exposure to water<sup>[67]</sup>. The multilayered PCB device used biodegradable metals such as Mg, W, and Zn for interconnects and PEO on a flexible sodium carboxymethylcellulose substrate. A plant-based biodegradable PCB was made from agricultural waste of natural cellulose<sup>[159]</sup>. The biocomposite used in the work

softens in contact with hot water or in high humidity. In another work, the performance of PCBs made from biodegradable cellulose acetate and PLA was compared with those created on Flame-Retardant Class 4 (FR-4) substrates<sup>[160]</sup>. Bharath *et al.*<sup>[161]</sup> explored rice husk-epoxy resin as a potential candidate for PCB. Although the performance of the PCBs and devices is far from that of the conventional devices, yet they hold promise to bring sustainability in electronics and make it environmentally friendly. For device applications, the functional lifetime is defined by the degradation time, thickness of material layers, and water permeability of the encapsulation materials. External stimulus triggers, namely, moisture, light, temperature, and mechanical force, have also been explored to degrade the materials in mostly non-aqueous environments.

Most of the initial devices using biodegradable materials used conventional manufacturing techniques of lithography, etching, and vapor or chemical deposition. Electrospinning and transfer techniques have also been explored but have been less successful when it comes to repeatability. Despite there are very few reports using additive manufacturing (AM) techniques to print biodegradable materials, discussion on this topic based on droplet-based printing techniques and 3D micro-additive manufacturing techniques has been initiated in a few papers<sup>[162-164]</sup>. PEDOT: PSS was converted into ink and printed using inkjet printer, which uses a piezoelectric nozzle and is a well-known drop-on-demand technique<sup>[164]</sup>. In a recent work by Williams *et al.*,<sup>[151]</sup> the emerging AM technique of aerosol jet printing was explored to fabricate an all-carbon thin-film transistor employing biodegradable material inks of nanocellulose and carbon nanotubes on paper substrate. A conductive paste of Zn, PVP, glycerol, and methanol was found to be suitable to create interconnects for screen printing. By combining screen printing with hot rolling and photonic sintering, a high conductivity of 60,213.6 S/m was achieved<sup>[28]</sup>. It was reported that among all printing methods, aerosol jet printing has the best resolution (line width >10 μm) and thus this technique offers better printing on a wide range of substrates and on 3D surfaces<sup>[164]</sup>.

## 8. End of life of electronics

Increasing electronic waste is an obstacle in the path of circular economy. Only 20% of e-waste gets recycled and a majority of it ends up in landfills, contributing to environmental problem. Researchers are exploring biodegradable materials to develop transient electronics in an effort to reduce e-waste. These devices have the capacity to dissolve in aqueous solutions to produce harmless products or to self-destruct themselves after operating for a predetermined period of time. The aim is to

counterbalance the negative trends conveyed by the short life cycle of electronics.

As discussed in this review paper, biodegradable metals generally convert into their oxides in aqueous solutions, and in some cases, they are non-reactive; therefore, they can be recycled back for use in another device, an example is liquid metal<sup>[165,166]</sup>. Researchers have experimented with recovering polymers back from the solution or degrading them enzymatically. In a previous study, an electrochromic display fabricated using PEDOT: PSS electrochromic layer, a gelatin-based electrolyte, and Au electrodes deposited on a cellulose diacetate substrate was tested for biodegradability study in accordance with the international standard ISO 14855. It was found that 79% of the device was able to degrade in 9 weeks by the microorganisms. The remaining 20% was cellulose diacetate and small amounts of PEDOT: PSS, glycerol, and gelatin<sup>[150]</sup>. In another study by Kwon *et al.*,<sup>[167]</sup> Ag composite with polycaprolactone (Ag-PCL) was used as a degradable electronic ink. The composite was embedded with enzymes to catalyze the hydrolytic degradation of PCL. This technique was useful to separate the electronic components, which can be recycled even after months of storage with no observable loss in performance. An all-carbon thin-film paper-based transistor was designed for controllable decomposition where efficiency to recapture graphene and carbon nanotubes was more than 95%. All the recycled materials could be reprinted in the form of new transistors with nearly identical performance to the thin film transistors (TFTs) created from new ink<sup>[151]</sup>.

Although researchers are working to make electronics more environmentally friendly by making them repairable, recyclable, or degradable so as to reduce the amount of e-waste, another significant challenge to focus on is incorporating the capability to quickly change a sensor or a component according to the need. This will eliminate the need to replace the entire device helping to further reduce the amount of waste produced and serving as both ecologically and economically viable options.

## 9. Challenges

Much effort has been put in studying and investigating the degradation of materials. However, the topics surrounding the breakdown of the emerging electronic materials and its effects on their performance are new. There are still many issues that need to be addressed so that the field can fully evolve.

- (i) One of the main challenges in biodegradable materials is their commercialization and acceptance by the industry. The synthesized biodegradable materials fall

short in comparison to their synthetic counterparts in technical and economic aspects.

- (ii) The biodegradability of various emerging materials has been tested and demonstrated only at the laboratory scale. It is essential to establish their biodegradability at the industrial scale and also set up standards for their commercial adoption.
- (iii) One major challenge is associated with synthesizing semiconducting and conducting biodegradable polymers that can find application in electronics and biomedical devices. To date, it is still challenging to retain the conductivity of biodegradable polymers while ensuring their functionality for the desired time. Two possible scenarios for solving the issue are either biomimicking the biodegradable natural materials for electronics properties or using novel chemistries to expand the library of biodegradable conducting polymers.
- (iv) One of the roadblocks for biodegradable materials is their application, especially in biomedical devices. The electroresponsive and tissue engineering materials have unknown biodegradation profile *in vitro* and *in vivo*. A lot of questions surrounding scaffold degradation and integration of cells or tissues with decomposing scaffold remain unanswered.

## 10. Conclusions and outlook

Development of biodegradable materials can help solve issues of e-waste, a growing problem that alone cannot be solved by recycling and reusing. This review summarizes the most current biodegradable materials currently being researched for their use in electronic devices and health-care solutions. The materials are comprehensively categorized and discussed according to their electrical conduction, namely, conductors, semiconductors, and insulators. Both natural and synthetic materials have been explored as substrates, electrodes, and active layers in many biodegradable devices. However, the field of biodegradable electronics is in its infancy, and the current biodegradable devices cannot compete with conventional devices in performance. Hence, there is a need to push research in the direction of exploring novel biodegradable materials that have better performance. The library also needs to expand to piezoelectric, piezoresistive, and energy materials to fully replace electronic circuitry in the future. Most biodegradation studies are limited to materials, and it is paramount to evaluate dissolution rates of materials with respect to their electrical performance. It is still unknown at what point biodegradable devices start to become unreliable. This review provides a comprehensive knowledge regarding the potential of fabricating green electronics that can be partially or fully degraded, thus paving way for sustainable electronics.

## Acknowledgments

None.

## Funding

The work is funded by the Villum Fonden grant (no: 37508).

## Conflict of interest

The authors declare no conflicts of interest.

## Author contributions

*Conceptualization:* Monisha Monisha and Shweta Agarwala

*Writing – original draft:* Monisha Monisha

*Writing – review & editing:* Monisha Monisha and Shweta Agarwala

All authors have read and agreed to the published version of the manuscript.

## References

1. Forti V, Balde CP, Kuehr R, *et al.*, 2020, The Global E-waste Monitor 2020: Quantities, Flows and the Circular Economy Potential. Available from: <https://ewastemonitor.info/gem-2020> [Last accessed on 2022 Jul 21].
2. Li R, Cheng H, Su Y, *et al.*, 2013, An analytical model of reactive diffusion for transient electronics. *Adv Funct Mater*, 23: 3106–3114.  
<https://doi.org/10.1002/adfm.201203088>
3. Yin L, Cheng H, Mao S, *et al.*, 2014, Dissolvable metals for transient electronics. *Adv Funct Mater*, 24: 645–658.  
<https://doi.org/10.1002/adfm.201301847>
4. Song G, Atrens A, 2003, Understanding magnesium corrosion a framework for improved alloy performance. *Adv Eng Mater*, 5: 837–858.  
<https://doi.org/10.1002/adem.200310405>
5. Li W, Liu Q, Zhang Y, *et al.*, 2020, Biodegradable materials and green processing for green electronics. *Adv Mater*, 32: 2001591.  
<https://doi.org/10.1002/adma.202001591>
6. Dagdeviren C, Hwang SW, Su Y, *et al.*, 2013, Transient, biocompatible electronics and energy harvesters based on ZnO. *Small*, 9: 3398–3404.  
<https://doi.org/10.1002/smll.201300146>
7. Oikawa H, 1975, Ellipsometric investigation of corrosion of deposited thin molybdenum film. *Jpn J Appl Phys*, 14: 629–635.  
<https://doi.org/10.1143/jjap.14.629>
8. Sherif ESM, Erasmus RM, Comins JD, 2010, *In situ* Raman spectroscopy and electrochemical techniques for studying corrosion and corrosion inhibition of iron in sodium chloride solutions. *Electrochim Acta*, 55: 3657–3663.  
<https://doi.org/10.1016/j.electacta.2010.01.117>
9. Kang SK, Hwang SW, Yu S, *et al.*, 2015, Biodegradable thin metal foils and spin-on glass materials for transient electronics. *Adv Funct Mater*, 25: 1789–1797.  
<https://doi.org/10.1002/adfm.201403469>
10. Hwang SW, Song JK, Huang X, *et al.*, 2014, High-performance biodegradable/transient electronics on biodegradable polymers. *Adv Mater*, 26: 3905–3911.  
<https://doi.org/10.1002/adma.201306050>
11. Kim BH, Kim JH, Persano L, *et al.*, 2017, Dry transient electronic systems by use of materials that sublime. *Adv Funct Mater*, 27: 1606008.  
<https://doi.org/10.1002/adfm.201606008>
12. Hwang SW, Park G, Edwards C, *et al.*, 2014, Dissolution chemistry and biocompatibility of single-crystalline silicon nanomembranes and associated materials for transient electronics. *ACS Nano*, 8: 5843–5851.  
<https://doi.org/10.1021/nn500847g>
13. Hwang SW, Park G, Cheng H, *et al.*, 2014, 25<sup>th</sup> anniversary article: Materials for high-performance biodegradable semiconductor devices. *Adv Mater*, 26: 1992–2000.  
<https://doi.org/10.1002/adma.201304821>
14. Yin L, Farimani AB, Min K, *et al.*, 2015, Mechanisms for hydrolysis of silicon nanomembranes as used in bioresorbable electronics. *Adv Mater*, 27: 1857–1864.  
<https://doi.org/10.1002/adma.201404579>
15. Lee YK, Yu KJ, Song E, *et al.*, 2017, Dissolution of monocrystalline silicon nanomembranes and their use as encapsulation layers and electrical interfaces in water-soluble electronics. *ACS Nano*, 11: 12562–12572.  
<https://doi.org/10.1021/acsnano.7b06697>
16. Yang SM, Shim JH, Cho HU, *et al.*, 2022, Hetero-integration of silicon nanomembranes with 2D materials for bioresorbable, wireless neurochemical system. *Adv Mater*, 34: 2108203.  
<https://doi.org/10.1002/adma.202108203>
17. Hwang SW, Tao H, Kim DH, *et al.*, 2012, A physically transient form of silicon electronics. *Science*, 337: 1640–1644.  
<https://doi.org/10.1126/science.1226325>
18. Seidel H, Csepregi L, Heuberger A, *et al.*, 1990, Anisotropic etching of crystalline silicon in alkaline solutions: II. Influence of dopants. *J Electrochem Soc*, 137: 3626–3632.  
<https://doi.org/10.1149/1.2086278>
19. Kang SK, Park G, Kim K, *et al.*, 2015, Dissolution chemistry

- and biocompatibility of silicon- and germanium-based semiconductors for transient electronics. *ACS Appl Mater Interfaces*, 7: 9297–9305.  
<https://doi.org/10.1021/acsami.5b02526>
20. Kang SK, Hwang SW, Cheng H, *et al.*, 2014, Dissolution behaviors and applications of silicon oxides and nitrides in transient electronics. *Adv Funct Mater*, 24: 4427–4434.  
<https://doi.org/10.1002/adfm.201304293>
21. Hwang SW, Kang SK, Huang X, *et al.*, 2015, Materials for programmed, functional transformation in transient electronic systems. *Adv Mater*, 27: 47–52.  
<https://doi.org/10.1002/adma.201403051>
22. Manivasagam G, Suwas S, 2014, Biodegradable Mg and Mg based alloys for biomedical implants. *Mater Sci Technol*, 30: 515–520.  
<https://doi.org/10.1179/1743284713Y.0000000500>
23. Patrick E, Orazem ME, Sanchez JC, *et al.*, 2011, Corrosion of tungsten microelectrodes used in neural recording applications. *J Neurosci Methods*, 198: 158–171.  
<https://doi.org/10.1016/j.jneumeth.2011.03.012>
24. Dahiya AS, Zumeit A, Christou A, *et al.*, 2022, High-performance n-channel printed transistors on biodegradable substrate for transient electronics. *Adv Electron Mater*, 8: 2200098.  
<https://doi.org/10.1002/aelm.202200098>
25. Feng S, Tian Z, Wang J, *et al.*, 2019, Laser sintering of Zn microparticles and its application in printable biodegradable electronics. *Adv Electron Mater*, 5: 1800693.  
<https://doi.org/10.1002/aelm.201800693>
26. Li J, Liu J, Lu W, *et al.*, 2021, Water-sintered transient nanocomposites used as electrical interconnects for dissolvable consumer electronics. *ACS Appl Mater Interfaces*, 13: 32136–32148.  
<https://doi.org/10.1021/acsami.1c07102>
27. Pandey V, Haider T, Jain P, *et al.*, 2020, Silk as a leading-edge biological macromolecule for improved drug delivery. *J Drug Deliv Sci Technol*, 55: 101294.  
<https://doi.org/10.1016/j.jddst.2019.101294>
28. Li J, Luo S, Liu J, *et al.*, 2018, Processing techniques for bioresorbable nanoparticles in fabricating flexible conductive interconnects. *Materials*, 11: 1102.  
<https://doi.org/10.3390/ma11071102>
29. Li H, Peng Q, Li X, *et al.*, 2014, Microstructures, mechanical and cytocompatibility of degradable Mg-Zn based orthopedic biomaterials. *Mater Des*, 58: 43–51.  
<https://doi.org/10.1016/j.matdes.2014.01.031>
30. Wang S, Guan S, Wang J, *et al.*, 2017, Fabrication and characterization of conductive poly (3,4-ethylenedioxythiophene) doped with hyaluronic acid/poly (l-lactic acid) composite film for biomedical application. *J Biosci Bioeng*, 123: 116–125.  
<https://doi.org/10.1016/j.jbiosc.2016.07.010>
31. Li L, Ge J, Guo B, *et al.*, 2014, *In situ* forming biodegradable electroactive hydrogels. *Polym Chem*, 5: 2880–2890.  
<https://doi.org/10.1039/C3PY01634J>
32. Tran RT, Thevenot P, Gyawali D, *et al.*, 2010, Synthesis and characterization of a biodegradable elastomer featuring a dual crosslinking mechanism. *Soft Matter*, 6: 2449–2461.  
<https://doi.org/10.1039/C001605E>
33. Jia X, Wang C, Ranganathan V, *et al.*, 2017, A biodegradable thin-film magnesium primary battery using silk fibroin-ionic liquid polymer electrolyte. *ACS Energy Lett*, 2: 831–836.  
<https://doi.org/10.1021/acsenerylett.7b00012>
34. Zhou J, Zhang R, Xu R, *et al.*, 2022, Super-assembled hierarchical cellulose aerogel-gelatin solid electrolyte for implantable and biodegradable zinc ion battery. *Adv Funct Mater*, 32: 2111406.  
<https://doi.org/10.1002/adfm.202111406>
35. Boutry CM, Nguyen A, Lawal QO, *et al.*, 2015, Fully Biodegradable Pressure Sensor, Viscoelastic Behavior of PGS Dielectric Elastomer Upon Degradation. 2015 IEEE SENSORS, 1-4 Nov.
36. Zhao D, Wu J, Chou DT, *et al.*, 2020, Visual hydrogen mapping sensor for noninvasive monitoring of bioresorbable magnesium implants *in vivo*. *JOM*, 72: 1851–1858.  
<https://doi.org/10.1007/s11837-020-04052-4>
37. Curry EJ, Ke K, Chorsi MT, *et al.*, 2018, Biodegradable piezoelectric force sensor. *Proc Natl Acad Sci*, 115: 909–914.  
<https://doi.org/10.1073/pnas.1710874115>
38. Suvarnaphaet P, Sasvimolkul S, Sukkasem C, *et al.*, 2019, *Biodegradable Electrode Patch Made of Graphene/PHA for ECG Detecting Applications*, 2019 12<sup>th</sup> Biomedical Engineering International Conference (BMEiCON), 19-22 Nov.
39. Zhu M, Jia C, Wang Y, *et al.*, 2018, Isotropic paper directly from anisotropic wood: Top-down green transparent substrate toward biodegradable electronics. *ACS Appl Mater Interfaces*, 10: 28566–28571.  
<https://doi.org/10.1021/acsami.8b08055>
40. Liu H, Jiang H, Du F, *et al.*, 2017, Flexible and degradable paper-based strain sensor with low cost. *ACS Sustain Chem Eng*, 5: 10538–10543.  
<https://doi.org/10.1021/acssuschemeng.7b02540>
41. Abdelkader AM, Karim N, Vallés C, *et al.*, 2017, Ultraflexible and robust graphene supercapacitors printed on textiles for

- wearable electronics applications. *2D Materials*, 4: 035016.  
<https://doi.org/10.1088/2053-1583/aa7d71>
42. Edupuganti V, Solanki R, 2016, Fabrication, characterization, and modeling of a biodegradable battery for transient electronics. *J Power Sources*, 336: 447–454.  
<https://doi.org/10.1016/j.jpowsour.2016.11.004>
43. Zhang Q, Liang Q, Rogers JA, 2020, Water-soluble energy harvester as a promising power solution for temporary electronic implants. *APL Mater*, 8: 120701.  
<https://doi.org/10.1063/5.0031151>
44. Krężel A, Maret W, 2016, The biological inorganic chemistry of zinc ions. *Arch Biochem Biophys*, 611: 3–19.  
<https://doi.org/10.1016/j.abb.2016.04.010>
45. Presuel-Moreno FJ, Jakab MA, Scully JR, 2005, Inhibition of the oxygen reduction reaction on copper with cobalt, cerium, and molybdate ions. *J Electrochem Soc*, 152: B376.  
<https://doi.org/10.1149/1.1997165>
46. Tolouei R, Harrison J, Paternoster C, *et al.*, 2016, The use of multiple pseudo-physiological solutions to simulate the degradation behavior of pure iron as a metallic resorbable implant: A surface-characterization study. *Phys Chem Chem Phys*, 18: 19637–19646.  
<https://doi.org/10.1039/C6CP02451C>
47. Zhang T, Tao Z, Chen J, 2014, Magnesium–air batteries: From principle to application. *Mater Horiz*, 1: 196–206.  
<https://doi.org/10.1039/C3MH00059A>
48. Yu X, Shou W, Mahajan BK, *et al.*, 2018, Materials, processes, and facile manufacturing for bioresorbable electronics: A review. *Adv Mater*, 30: 1707624.  
<https://doi.org/10.1002/adma.201707624>
49. Fernandes C, Taurino I, 2022, Biodegradable molybdenum (Mo) and tungsten (W) devices: One step closer towards fully-transient biomedical implants. *Sensors (Basel)*, 22: 3062.  
<https://doi.org/10.3390/s22083062>
50. Laing PG, 1979, Clinical experience with prosthetic materials: Historical perspectives, current problems, and future directions. USA: ASTM Int, 199–211.  
<https://doi.org/10.1520/STP35945S>
51. Cao Y, Wang S, Lv J, *et al.*, 2022, Fully physically transient volatile memristor based on mg/magnesium oxide for biodegradable neuromorphic electronics. *IEEE Trans Electron Devices*, 69: 3118–3123.  
<https://doi.org/10.1109/TED.2022.3166868>
52. Xiang W, Hongmei L, Xinlin L, *et al.*, 2007, Effect of cooling rate and composition on microstructures and properties of Zn-Mg alloys. *Trans Nonferrous Metals Soc China*, 17: 122–125.
53. Han WB, Yang SM, Rajaram K, *et al.*, 2022, Materials and fabrication strategies for biocompatible and biodegradable conductive polymer composites toward bio-integrated electronic systems. *Adv Sustain Syst*, 6: 2100075.  
<https://doi.org/10.1002/adsu.202100075>
54. Machado JM, Karasz FE, Lenz RW, 1988, Electrically conducting polymer blends. *Polymer*, 29: 1412–1417.  
[https://doi.org/10.1016/0032-3861\(88\)90304-7](https://doi.org/10.1016/0032-3861(88)90304-7)
55. Cao Y, Smith P, Heeger AJ, 1992, Counter-ion induced processibility of conducting polyaniline and of conducting polyblends of polyaniline in bulk polymers. *Synth Met*, 48: 91–97.  
[https://doi.org/10.1016/0379-6779\(92\)90053-L](https://doi.org/10.1016/0379-6779(92)90053-L)
56. Knackstedt MA, Roberts AP, 1996, Morphology and macroscopic properties of conducting polymer blends. *Macromolecules*, 29: 1369–1371.  
<https://doi.org/10.1021/ma951295h>
57. Worfolk BJ, Andrews SC, Park S, *et al.*, 2015, Ultrahigh electrical conductivity in solution-sheared polymeric transparent films. *Proc Natl Acad Sci*, 112: 14138–14143.  
<https://doi.org/10.1073/pnas.1509958112>
58. Wang YF, Sekine T, Takeda Y, *et al.*, 2020, Fully printed PEDOT: PSS-based temperature sensor with high humidity stability for wireless healthcare monitoring. *Sci Rep*, 10: 2467.  
<https://doi.org/10.1038/s41598-020-59432-2>
59. Shi G, Rouabhia M, Wang Z, *et al.*, 2004, A novel electrically conductive and biodegradable composite made of polypyrrole nanoparticles and polylactide. *Biomaterials*, 25: 2477–2488.  
<https://doi.org/10.1016/j.biomaterials.2003.09.032>
60. Pradhan S, Yadavalli VK, 2021, Photolithographically printed flexible silk/PEDOT: PSS temperature sensors. *ACS Appl Electron Mater*, 3: 21–29.  
<https://doi.org/10.1021/acsaelm.0c01017>
61. Lawes S, Sun Q, Lushington A, *et al.*, 2017, Inkjet-printed silicon as high performance anodes for Li-ion batteries. *Nano Energy*, 36: 313–321.  
<https://doi.org/10.1016/j.nanoen.2017.04.041>
62. Li M, Guo Y, Wei Y, *et al.*, 2006, Electrospinning polyaniline-contained gelatin nanofibers for tissue engineering applications. *Biomaterials*, 27: 2705–2715.  
<https://doi.org/10.1016/j.biomaterials.2005.11.037>
63. Jeong SI, Jun ID, Choi MJ, *et al.*, 2008, Development of electroactive and elastic nanofibers that contain polyaniline and poly(L-lactide-co-ε-caprolactone) for the control of cell adhesion. *Macromol Biosci*, 8: 627–637.

- <https://doi.org/10.1002/mabi.200800005>
64. Subramanian A, Krishnan UM, Sethuraman S, 2012, Axially aligned electrically conducting biodegradable nanofibers for neural regeneration. *J Mater Sci Mater Med*, 23: 1797–1809.  
<https://doi.org/10.1007/s10856-012-4654-y>
65. Mahajan BK, Ludwig B, Shou W, *et al.*, 2018, Aerosol printing and photonic sintering of bioresorbable zinc nanoparticle ink for transient electronics manufacturing. *Sci China Inf Sci*, 61: 060412.  
<https://doi.org/10.1007/s11432-018-9366-5>
66. Li J, Xu H, Zhang Z, *et al.*, 2020, Anhydride-assisted spontaneous room temperature sintering of printed bioresorbable electronics. *Adv Funct Mater*, 30: 1905024.  
<https://doi.org/10.1002/adfm.201905024>
67. Huang X, Liu Y, Hwang SW, *et al.*, 2014, Biodegradable materials for multilayer transient printed circuit boards. *Adv Mater*, 26: 7371–7377.  
<https://doi.org/10.1002/adma.201403164>
68. Iwai H, Ohmi SI, 2002, Silicon integrated circuit technology from past to future. *Microelectron Reliab*, 42: 465–491.  
[https://doi.org/10.1016/S0026-2714\(02\)00032-X](https://doi.org/10.1016/S0026-2714(02)00032-X)
69. Snell AJ, Spear WE, Le Comber PG, *et al.*, 1981, Application of amorphous silicon field effect transistors in integrated circuits. *Appl Phys A*, 26: 83–86.  
<https://doi.org/10.1007/BF00616653>
70. Bowman DR, Hammond RB, Dutton RW, 1985, Polycrystalline-silicon integrated photoconductors for picosecond pulsing and gating. *IEEE Electron Device Lett*, 6: 502–504.  
<https://doi.org/10.1109/EDL.1985.26209>
71. Guha S, Yang J, Banerjee A, 2000, Amorphous silicon alloy photovoltaic research—present and future. *Prog Photovolt: Res Appl*, 8: 141–150.  
[https://doi.org/10.1002/\(SICI\)1099-159X\(200001/02\)8:1<141:AID-PIP305>3.0.CO;2-I](https://doi.org/10.1002/(SICI)1099-159X(200001/02)8:1<141:AID-PIP305>3.0.CO;2-I)
72. Kang SK, Koo J, Lee YK, *et al.*, 2018, Advanced materials and devices for bioresorbable electronics. *Acc Chem Res*, 51: 988–998.  
<https://doi.org/10.1021/acs.accounts.7b00548>
73. Fu KK, Wang Z, Dai J, *et al.*, 2016, Transient electronics: Materials and devices. *Chem Mater*, 28: 3527–3539.  
<https://doi.org/10.1021/acs.chemmater.5b04931>
74. Li R, Wang L, Kong D, *et al.*, 2018, Recent progress on biodegradable materials and transient electronics. *Bioact Mater*, 3: 322–333.  
<https://doi.org/10.1016/j.bioactmat.2017.12.001>
75. Li R, Wang L, Yin L, 2018, Materials and devices for biodegradable and soft biomedical electronics. *Materials*, 11: 2108.
76. Madrigal MM, Giannotti MI, Oncins G, *et al.*, 2013, Bioactive nanomembranes of semiconductor polythiophene and thermoplastic polyurethane: Thermal, nanostructural and nanomechanical properties. *Polym Chem*, 4: 568–583.  
<https://doi.org/10.1039/c2py20654d>
77. Pérez-Madrigal MM, Giannotti MI, Armelin E, *et al.*, 2014, Electronic, electric and electrochemical properties of bioactive nanomembranes made of polythiophene: Thermoplastic polyurethane. *Polym Chem*, 5: 1248–1257.  
<https://doi.org/10.1039/C3PY01313H>
78. Lei T, Guan M, Liu J, *et al.*, 2017, Biocompatible and totally disintegrable semiconducting polymer for ultrathin and ultralightweight transient electronics. *Proc Natl Acad Sci*, 114: 5107–5112.  
<https://doi.org/10.1073/pnas.1701478114>
79. Xu C, Huang Y, Yopez G, *et al.*, 2016, Development of dopant-free conductive bioelastomers. *Sci Rep*, 6: 34451.  
<https://doi.org/10.1038/srep34451>
80. Mostert AB, Powell BJ, Pratt FL, *et al.*, 2012, Role of semiconductivity and ion transport in the electrical conduction of melanin. *Proc Natl Acad Sci*, 109: 8943–8947.  
<https://doi.org/10.1073/pnas.1119948109>
81. Bettinger CJ, Bruggeman JP, Misra A, *et al.*, 2009, Biocompatibility of biodegradable semiconducting melanin films for nerve tissue engineering. *Biomaterials*, 30: 3050–3057.  
<https://doi.org/10.1016/j.biomaterials.2009.02.018>
82. Irimia-Vladu M, Głowacki ED, Troshin PA, *et al.*, 2012, Indigo a natural pigment for high performance ambipolar organic field effect transistors and circuits. *Adv Mater*, 24: 375–380.  
<https://doi.org/10.1002/adma.201102619>
83. Ramachandran GK, Tomfohr JK, Li J, *et al.*, 2003, Electron transport properties of a carotene molecule in a metal-(single molecule)-metal junction. *J Phys Chem B*, 107: 6162–6169.  
<https://doi.org/10.1021/jp0343786>
84. Irimia-Vladu M, Troshin PA, Reisinger M, *et al.*, 2010, Biocompatible and biodegradable materials for organic field-effect transistors. *Adv Funct Mater*, 20: 4069–4076.  
<https://doi.org/10.1002/adfm.201001031>
85. Guo B, Finne-Wistrand A, Albertsson AC, 2010, Enhanced electrical conductivity by macromolecular architecture: Hyperbranched electroactive and degradable block copolymers based on poly( $\epsilon$ -caprolactone) and aniline

- pentamer. *Macromolecules*, 43: 4472–4480.  
<https://doi.org/10.1021/ma100530k>
86. Cui H, Liu Y, Deng M, *et al.*, 2012, Synthesis of biodegradable and electroactive tetraaniline grafted poly(ester amide) copolymers for bone tissue engineering. *Biomacromolecules*, 13: 2881–2889.  
<https://doi.org/10.1021/bm300897j>
87. Champion JA, Walker A, Mitragotri S, 2008, Role of particle size in phagocytosis of polymeric microspheres. *Pharm Res*, 25: 1815–1821.  
<https://doi.org/10.1007/s11095-008-9562-y>
88. Temenoff JS, Mikos AG, 2008, *Biomaterials: The Intersection of Biology and Materials Science*. Pearson/Prentice Hall, London, United Kingdom.
89. Shou W, Mahajan BK, Ludwig B, *et al.*, 2017, Low-cost manufacturing of bioresorbable conductors by evaporation–condensation-mediated laser printing and sintering of Zn nanoparticles. *Adv Mater*, 29: 1700172.  
<https://doi.org/10.1002/adma.201700172>
90. Feng S, Cao S, Tian Z, *et al.*, 2019, Maskless patterning of biodegradable conductors by selective laser sintering of microparticle inks and its application in flexible transient electronics. *ACS Appl Mater Interfaces*, 11: 45844–45852.  
<https://doi.org/10.1021/acsami.9b14431>
91. Shin SR, Farzad R, Tamayol A, *et al.*, 2016, A bioactive carbon nanotube-based ink for printing 2D and 3D flexible electronics. *Adv Mater*, 28: 3280–3289.  
<https://doi.org/10.1002/adma.201506420>
92. Leng T, Huang X, Chang K, *et al.*, 2016, Graphene nanoflakes printed flexible meandered-line dipole antenna on paper substrate for low-cost RFID and sensing applications. *IEEE Antennas Wirel Propag Lett*, 15: 1565–1568.  
<https://doi.org/10.1109/LAWP.2016.2518746>
93. Deshmukh K, Ahamed MB, Deshmukh RR, *et al.*, 2017, Newly developed biodegradable polymer nanocomposites of cellulose acetate and Al<sub>2</sub>O<sub>3</sub> nanoparticles with enhanced dielectric performance for embedded passive applications. *J Mater Sci Mater Electron*, 28: 973–986.  
<https://doi.org/10.1007/s10854-016-5616-9>
94. Zeng X, Deng L, Yao Y, *et al.*, 2016, Flexible dielectric papers based on biodegradable cellulose nanofibers and carbon nanotubes for dielectric energy storage. *J Mater Chem C*, 4: 6037–6044.  
<https://doi.org/10.1039/C6TC01501H>
95. Mukai Y, Suh M, 2020, Relationships between structure and microwave dielectric properties in cotton fabrics. *Mater Res Express*, 7: 015105.  
<https://doi.org/10.1088/2053-1591/ab653c>
96. Liu Z, Liang T, Xin Y, *et al.*, 2021, Natural bamboo leaves as dielectric layers for flexible capacitive pressure sensors with adjustable sensitivity and a broad detection range. *RSC Adv*, 11: 17291–17300.  
<https://doi.org/10.1039/D1RA03207K>
97. Larguech S, Triki A, Ramachandran M, *et al.*, 2021, Dielectric properties of jute fibers reinforced poly(lactic acid)/poly(butylene succinate) blend matrix. *J Polym Environ*, 29: 1240–1256.  
<https://doi.org/10.1007/s10924-020-01927-0>
98. Ivanovska A, Cerovic D, Tadic N, *et al.*, 2019, Sorption and dielectric properties of jute woven fabrics: Effect of chemical composition. *Ind Crops Prod*, 140: 111632.  
<https://doi.org/10.1016/j.indcrop.2019.111632>
99. Doddashamachar M, Setty RNV, Reddy MVH, *et al.*, 2022, Dielectric properties of banana fiber filled polypropylene composites: Effect of coupling agent. *Fibers Polym*, 23: 1387–1395.  
<https://doi.org/10.1007/s12221-022-4395-6>
100. Joseph S, Thomas S, 2008, Electrical properties of banana fiber-reinforced phenol formaldehyde composites. *J Appl Polym Sci*, 109: 256–263.  
<https://doi.org/10.1002/app.27452>
101. Hemstreet JM, 1982, Dielectric constant of cotton. *J Electrostat*, 13: 345–353.  
[https://doi.org/10.1016/0304-3886\(82\)90052-3](https://doi.org/10.1016/0304-3886(82)90052-3)
102. Jayamani E, Hamdan S, Rahman MR, *et al.*, 2014, Comparative study of dielectric properties of hybrid natural fiber composites. *Proc Eng*, 97: 536–544.  
<https://doi.org/10.1016/j.proeng.2014.12.280>
103. Boutry CM, Nguyen A, Lawal QO, *et al.*, 2015, A sensitive and biodegradable pressure sensor array for cardiovascular monitoring. *Adv Mater*, 27: 6954–6961.  
<https://doi.org/10.1002/adma.201502535>
104. Barone C, Maccagnani P, Dinelli F, *et al.*, 2022, Electrical conduction and noise spectroscopy of sodium-alginate gold-covered ultrathin films for flexible green electronics. *Sci Rep*, 12: 9861.  
<https://doi.org/10.1038/s41598-022-14030-2>
105. Guo J, Liu J, Yang B, *et al.*, 2015, Low-voltage transient/biodegradable transistors based on free-standing sodium alginate membranes. *IEEE Electron Device Lett*, 36: 576–578.  
<https://doi.org/10.1109/LED.2015.2424982>
106. Kumar R, Ranwa S, Kumar G, 2020, Biodegradable flexible substrate based on chitosan/PVP blend polymer for disposable electronics device applications. *J Phys Chem B*, 124: 149–155.  
<https://doi.org/10.1021/acs.jpcc.9b08897>

107. Peng X, Dong K, Zhang Y, *et al.*, 2022, Sweat-permeable, biodegradable, transparent and self-powered chitosan-based electronic skin with ultrathin elastic gold nanofibers. *Adv Funct Mater*, 32: 2112241.  
<https://doi.org/10.1002/adfm.202112241>
108. Baumgartner M, Hartmann F, Drack M, *et al.*, 2020, Resilient yet entirely degradable gelatin-based biogels for soft robots and electronics. *Nat Mater*, 19: 1102–1109.  
<https://doi.org/10.1038/s41563-020-0699-3>
109. Wang C, Yokota T, Someya T, 2021, Natural biopolymer-based biocompatible conductors for stretchable bioelectronics. *Chem Rev*, 121: 2109–2146.  
<https://doi.org/10.1021/acs.chemrev.0c00897>
110. Yang Y, Sun H, Zhao X, *et al.*, 2022, High-mobility fungus-triggered biodegradable ultraflexible organic transistors. *Adv Sci*, 9: 2105125.  
<https://doi.org/10.1002/advs.202105125>
111. Hwang SW, Lee CH, Cheng H, *et al.*, 2015, Biodegradable elastomers and silicon nanomembranes/nanoribbons for stretchable, transient electronics, and biosensors. *Nano Lett*, 15: 2801–2808.  
<https://doi.org/10.1021/nl503997m>
112. Jung YH, Chang TH, Zhang H, *et al.*, 2015, High-performance green flexible electronics based on biodegradable cellulose nanofibril paper. *Nat Commun*, 6: 7170.  
<https://doi.org/10.1038/ncomms8170>
113. Jin SH, Kang SK, Cho IT, *et al.*, 2015, Water-soluble thin film transistors and circuits based on amorphous indium–gallium–zinc oxide. *ACS Appl Mater Interfaces*, 7: 8268–8274.  
<https://doi.org/10.1021/acsami.5b00086>
114. Liu Q, Jiang L, Shi R, *et al.*, 2012, Synthesis, preparation, *in vitro* degradation, and application of novel degradable bioelastomers a review. *Prog Polym Sci*, 37: 715–765.  
<https://doi.org/10.1016/j.progpolymsci.2011.11.001>
115. Nijst CL, Bruggeman JP, Karp JM, *et al.*, 2007, Synthesis and characterization of photocurable elastomers from poly(glycerol-co-sebacate). *Biomacromolecules*, 8: 3067–3073.  
<https://doi.org/10.1021/bm070423u>
116. Benfenati V, Toffanin S, Capelli R, *et al.*, 2010, A silk platform that enables electrophysiology and targeted drug delivery in brain astroglial cells. *Biomaterials*, 31: 7883–7891.  
<https://doi.org/10.1016/j.biomaterials.2010.07.013>
117. Tao H, Hwang SW, Marelli B, *et al.*, 2014, Silk-based resorbable electronic devices for remotely controlled therapy and *in vivo* infection abatement. *Proc Natl Acad Sci*, 111: 17385–17389.  
<https://doi.org/10.1073/pnas.1407743111>
118. Zhu M, Liu Y, Jiang F, *et al.*, 2020, Combined silk fibroin microneedles for insulin delivery. *ACS Biomater Sci Eng*, 6: 3422–3429.  
<https://doi.org/10.1021/acsbiomaterials.0c00273>
119. Kim HJ, Kim JH, Jun KW, *et al.*, 2016, Silk nanofiber-networked bio-triboelectric generator: silk bio-TEG. *Adv Energy Mater*, 6: 1502329.  
<https://doi.org/10.1002/aenm.201502329>
120. Mi HY, Li H, Jing X, *et al.*, 2020, Silk and silk composite aerogel-based biocompatible triboelectric nanogenerators for efficient energy harvesting. *Ind Eng Chem Res*, 59: 12399–12408.  
<https://doi.org/10.1021/acs.iecr.0c01117>
121. Ye C, Dong S, Ren J, *et al.*, 2019, Ultrastable and high-performance silk energy harvesting textiles. *Nanomicro Lett*, 12: 12.  
<https://doi.org/10.1007/s40820-019-0348-z>
122. Lee CP, Lai KY, Lin CA, *et al.*, 2017, A paper-based electrode using a graphene dot/PEDOT: PSS composite for flexible solar cells. *Nano Energy*, 36: 260–267.  
<https://doi.org/10.1016/j.nanoen.2017.04.044>
123. Castro-Hermosa S, Dagar J, Marsella A, *et al.*, 2017, Perovskite solar cells on paper and the role of substrates and electrodes on performance. *IEEE Electron Device Lett*, 38: 1278–1281.  
<https://doi.org/10.1109/LED.2017.2735178>
124. Jia C, Li T, Chen C, *et al.*, 2017, Scalable, anisotropic transparent paper directly from wood for light management in solar cells. *Nano Energy*, 36: 366–373.  
<https://doi.org/10.1016/j.nanoen.2017.04.059>
125. Jayaraman E, Iyer SS, 2020, Organic photovoltaic modules built on paper substrates. *Adv Mater Technol*, 5: 2000664.  
<https://doi.org/10.1002/admt.202000664>
126. Cinti S, Colozza N, Cacciotti I, *et al.*, 2018, Electroanalysis moves towards paper-based printed electronics: Carbon black nanomodified inkjet-printed sensor for ascorbic acid detection as a case study. *Sens Actuators B Chem*, 265: 155–160.  
<https://doi.org/10.1016/j.snb.2018.03.006>
127. Hui CY, Liu M, Li Y, *et al.*, 2018, A paper sensor printed with multifunctional bio/nano materials. *Angew Chem Int Ed*, 57: 4549–4553.  
<https://doi.org/10.1002/anie.201712903>
128. Tao LQ, Zhang KN, Tian H, *et al.*, 2017, Graphene-paper pressure sensor for detecting human motions. *ACS Nano*, 11: 8790–8795.

- <https://doi.org/10.1021/acsnano.7b02826>
129. Carvalho JT, Dubceac V, Grey P, *et al.*, 2019, Fully printed zinc oxide electrolyte-gated transistors on paper. *Nanomaterials*, 9: 169.
130. Lee CJ, Chang YC, Wang LW, *et al.*, 2019, Biodegradable materials for organic field-effect transistors on a paper substrate. *IEEE Electron Device Lett*, 40: 236–239.  
<https://doi.org/10.1109/LED.2018.2890618>
131. Raghuvanshi V, Bharti D, Mahato AK, *et al.*, 2019, Solution-processed organic field-effect transistors with high performance and stability on paper substrates. *ACS Appl Mater Interfaces*, 11: 8357–8364.  
<https://doi.org/10.1021/acsnano.7b02826>
132. Zschieschang U, Klauk H, 2019, Organic transistors on paper: A brief review. *J Mater Chem C*, 7: 5522–5533.  
<https://doi.org/10.1039/C9TC00793H>
133. Mohammadifar M, Yazgan I, Zhang J, *et al.*, 2018, Green biobatteries: Hybrid paper-polymer microbial fuel cells. *Adv Sustain Syst*, 2: 1800041.  
<https://doi.org/10.1002/adsu.201800041>
134. Kim S, Georgiadis A, Tentzeris MM, 2018, Design of inkjet-printed RFID-based sensor on paper: single- and dual-tag sensor topologies. *Sensors (Basel)*, 18: 1958.
135. Wang Y, Yan C, Cheng SY, *et al.*, 2019, Flexible RFID tag metal antenna on paper-based substrate by inkjet printing technology. *Adv Funct Mater*, 29: 1902579.  
<https://doi.org/10.1002/adfm.201902579>
136. Zhu H, Fang Z, Preston C, *et al.*, 2014, Transparent paper: Fabrications, properties, and device applications. *Energy Environ Sci*, 7: 269–287.  
<https://doi.org/10.1039/C3EE43024C>
137. Hsieh MC, Kim C, Nogi M, *et al.*, 2013, Electrically conductive lines on cellulose nanopaper for flexible electrical devices. *Nanoscale*, 5: 9289–9295.  
<https://doi.org/10.1039/C3NR01951A>
138. Miller RA, Brady JM, Cutright DE, 1977, Degradation rates of oral resorbable implants (polylactates and polyglycolates): Rate modification with changes in PLA/PGA copolymer ratios. *J Biomed Mater Res*, 11: 711–719.  
<https://doi.org/10.1002/jbm.820110507>
139. Najafabadi AH, Tamayol A, Annabi N, *et al.*, 2014, Biodegradable nanofibrous polymeric substrates for generating elastic and flexible electronics. *Adv Mater*, 26: 5823–5830.  
<https://doi.org/10.1002/adma.201401537>
140. Luoma E, Välimäki M, Ollila J, *et al.*, 2022, Bio-based polymeric substrates for printed hybrid electronics. *Polymers (Basel)*, 14: 1863.  
<https://doi.org/10.3390/polym14091863>
141. Hao XP, Zhang CW, Zhang XN, *et al.*, 2022, Healable, recyclable, and multifunctional soft electronics based on biopolymer hydrogel and patterned liquid metal. *Small*, 18: 2201643.  
<https://doi.org/10.1002/smll.202201643>
142. Moon J, Diaz V, Patel D, *et al.*, 2022, Dissolvable conducting polymer supercapacitor for transient electronics. *Org Electron*, 101: 106412.  
<https://doi.org/10.1016/j.orgel.2021.106412>
143. Gao Y, Zhang Y, Wang X, *et al.*, 2017, Moisture-triggered physically transient electronics. *Sci Adv*, 3: e1701222.  
<https://doi.org/10.1126/sciadv.1701222>
144. Park CW, Kang SK, Hernandez HL, *et al.*, 2015, Thermally triggered degradation of transient electronic devices. *Adv Mater*, 27: 3783–3788.  
<https://doi.org/10.1002/adma.201501180>
145. Hernandez HL, Kang SK, Lee OP, *et al.*, 2014, Triggered transience of metastable poly(phthalaldehyde) for transient electronics. *Adv Mater*, 26: 7637–7642.  
<https://doi.org/10.1002/adma.201403045>
146. Kang SK, Murphy RK, Hwang SW, *et al.*, 2016, Bioresorbable silicon electronic sensors for the brain. *Nature*, 530: 71–76.  
<https://doi.org/10.1038/nature16492>
147. Park S, Yun WM, Kim LH, *et al.*, 2013, Inorganic/organic multilayer passivation incorporating alternating stacks of organic/inorganic multilayers for long-term air-stable organic light-emitting diodes. *Org Electron*, 14: 3385–3391.  
<https://doi.org/10.1016/j.orgel.2013.09.045>
148. Feiner R, Fleischer S, Shapira A, *et al.*, 2018, Multifunctional degradable electronic scaffolds for cardiac tissue engineering. *J Control Release*, 281: 189–195.  
<https://doi.org/10.1016/j.jconrel.2018.05.023>
149. Son D, Lee J, Lee DJ, *et al.*, 2015, Bioresorbable electronic stent integrated with therapeutic nanoparticles for endovascular diseases. *ACS Nano*, 9: 5937–5946.  
<https://doi.org/10.1021/acsnano.5b00651>
150. Pietsch M, Schliske S, Held M, *et al.*, 2020, Biodegradable inkjet-printed electrochromic display for sustainable short-lifecycle electronics. *J Mater Chem C*, 8: 16716–16724.  
<https://doi.org/10.1039/D0TC04627B>
151. Williams NX, Bullard G, Brooke N, *et al.*, 2021, Printable and recyclable carbon electronics using crystalline nanocellulose dielectrics. *Nat Electron*, 4: 261–268.  
<https://doi.org/10.1038/s41928-021-00574-0>
152. Nadeau P, El-Damak D, Glettig D, *et al.*, 2017, Prolonged energy harvesting for ingestible devices. *Nat Biomed Eng*, 1: 22.

- <https://doi.org/10.1038/s41551-016-0022>
153. Mei T, Wang C, Liao M, *et al.*, 2021, A biodegradable and rechargeable fiber battery. *J Mater Chem A*, 9: 10104–10109.  
<https://doi.org/10.1039/D1TA01507A>
154. Wang Z, Li X, Yang Z, *et al.*, 2021, Fully transient stretchable fruit-based battery as safe and environmentally friendly power source for wearable electronics. *EcoMat*, 3: e12073.  
<https://doi.org/10.1002/eom2.12073>
155. Sun J, Wang H, Song F, *et al.*, 2018, Physically transient threshold switching device based on magnesium oxide for security application. *Small*, 14: 1800945.  
<https://doi.org/10.1002/smll.201800945>
156. Lu L, Yang Z, Meacham K, *et al.*, 2018, Biodegradable monocrystalline silicon photovoltaic microcells as power supplies for transient biomedical implants. *Adv Energy Mater*, 8: 1703035.  
<https://doi.org/10.1002/aenm.201703035>
157. Song F, Wang H, Sun J, *et al.*, 2018, ZnO-based physically transient and bioresorbable memory on silk protein. *IEEE Electron Device Lett*, 39: 31–34.  
<https://doi.org/10.1109/LED.2017.2774842>
158. Wang H, Zhu B, Ma X, *et al.*, 2016, Physically transient resistive switching memory based on silk protein. *Small*, 12: 2715–2719.  
<https://doi.org/10.1002/smll.201502906>
159. Guna VK, Murugesan G, Basavarajaiah BH, *et al.*, 2016, Plant-based completely biodegradable printed circuit boards. *IEEE Trans Electron Devices*, 63: 4893–4898.  
<https://doi.org/10.1109/TED.2016.2619983>
160. Géczy A, Nagy D, Hajdu I, *et al.*, 2015, Investigating Mechanical Performance of PLA and CA Biodegradable Printed Circuit Boards, 2015 IEEE 21<sup>st</sup> International Symposium for Design and Technology in Electronic Packaging (SIITME), 2015 22–25 Oct. 201545–49.
161. Bharath KN, Madhu P, Gowda TGY, *et al.*, 2020, A novel approach for development of printed circuit board from biofiber based composites. *Polym Compos*, 41: 4550–4558.  
<https://doi.org/10.1002/pc.25732>
162. Abdolmaleki H, Kidmose P, Agarwala S, 2021, Droplet-based techniques for printing of functional inks for flexible physical sensors. *Adv Mater*, 33: 2006792.  
<https://doi.org/10.1002/adma.202006792>
163. Vaezi M, Seitz H, Yang S, 2013, A review on 3D micro-additive manufacturing technologies. *Int J Adv Manuf Technol*, 67: 1721–1754.  
<https://doi.org/10.1007/s00170-012-4605-2>
164. Saengchairat N, Tran T, Chua CK, 2017, A review: Additive manufacturing for active electronic components. *Virtual Phys Prototyp*, 12: 31–46.  
<https://doi.org/10.1080/17452759.2016.1253181>
165. Teng L, Ye S, Handschuh-Wang S, *et al.*, 2019, Liquid metal-based transient circuits for flexible and recyclable electronics. *Adv Funct Mater*, 29: 1808739.  
<https://doi.org/10.1002/adfm.201808739>
166. Tavakoli M, Lopes PA, Hajalilou A, *et al.*, 2022, 3R Electronics: Scalable fabrication of resilient, repairable, and recyclable soft-matter electronics. *Adv Mater*, 34: 2203266.  
<https://doi.org/10.1002/adma.202203266>
167. Kwon J, DelRe C, Kang P, *et al.*, 2022, Conductive ink with circular life cycle for printed electronics. *Adv Mater*, 34: 2202177.  
<https://doi.org/10.1002/adma.202202177>